Cancer Cell International

RESEARCH

Open Access

miR-484 sensitizes in IDH-wild and IDH-mutant glioblastoma cells to temozolomide by inhibiting oncogenic FOXM1 signaling

Nursultan Nurdinov[1,2,3], Ahsen Güler[1,2], Serhat Albayrak[2,4], Gizem Kursunluoglu[5], Halil Ulutabanca[6], Venhar Cınar[1,2,7], Mehmet Memis[2,4], Serife Erdem[2,8], Omer Aydın[5,9], Elif Funda Sener[1,2], Serpil Taheri[1,2], Bulent Ozpolat[10*] and Zuhal Hamurcu[1,2*]

Abstract

Background Glioblastoma (GBM) is the most diagnosed primary brain tumor with an extremely poor survival rate. Emerging evidence suggests that miRNAs are involved in GBM tumorigenesis. miR-484 was highly expressed in glioma cells and enhanced cell migration, and invasion. However, the role of miR-484 in GBM and its downstream targets are not well understood.

Methods We analyzed miR-484 expression in GBM patient tissue samples (IDH wild-type and IDH-mutant) and cell lines via Real-Time PCR. In GBM cells transfected with inhibitor- and mimic-miR-484, we investigated cell proliferation, migration, invasion, cell cycle, and apoptosis. Additionally, protein expression of FOXM1 and its downstream targets were investigated. RNA-seq analysis was performed on mimic-miR-484-transfected U87-MG and IDH1-mutant-U87 cells.

Results miR-484 expression was higher in IDH-mutant patient tumors compared to IDH1-wild type patient tumors. Ectopic expression of miR-484 suppressed cell proliferation, colony formation, migration and invasion, and induced apoptosis in GBM cells. Furthermore, we found that miR-484 suppresses FOXM1 and its downstream targets including Integrin-β1/FAK/Src and Cyclin-D and PARP, all of which have been shown to be potential therapeutic targets in GBM cells. In addition, expression of miR-484 enhanced TMZ-induced FOXM1 downregulation in GBM.

Conclusion Our findings suggest for the first time that miR-484 act as a tumor suppressor in IDH1-wild type and mutant GBM cells by targeting FOXM1 oncogenic transcription factor and its downstream in GBM cells. Therefore, miR-484-based treatment may provide a new avenue for controlling GMB growth and progression and may enhance the therapeutic efficacy of TMZ.

Trial registry: decision no: 2019/247.

*Correspondence:
Bulent Ozpolat
bozpolat@ou.edu
Zuhal Hamurcu
zhamurcu@erciyes.edu.tr

Full list of author information is available at the end of the article

Keywords miR-484, Brain cancer, Glioblastoma multiforme, GBM, FOXM1, Proliferation, Invasion, TMZ, Apoptosis, Resistance, siRNA

Graphical abstract

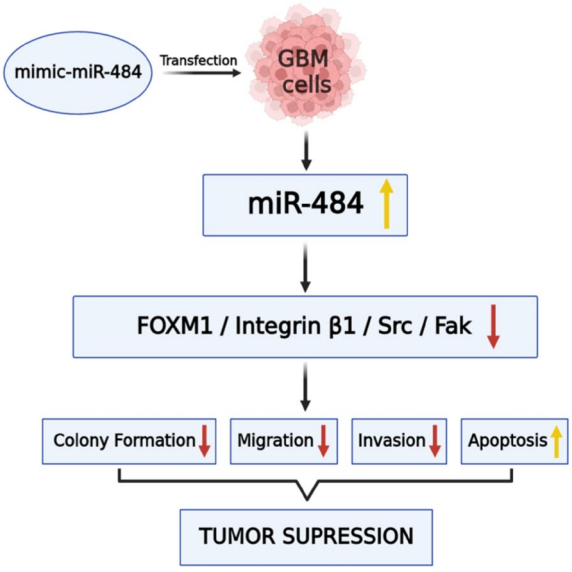

Introduction

Gliomas are diverse group cancers arising from glial cells in the brain and spinal cord. The World Health Organization (WHO) has classified gliomas into) lower-grade gliomas (grade II and grade III) and glioblastoma (GBM; grade IV). GBM is the most common primary brain tumor and about 60% of all gliomas are GBM. Based on the mutational status of isocitrate dehydrogenase (IDH) gene, GBM is classified as [1] IDH-wild type and [2] IDH-mutant GBM by the WHO (CNS 2016) [1–3]. The 2021 WHO Classification of CNS Tumours, was based on Isocitrate Dehydrogenase (IDH1/2) mutation status as the separation of diffuse gliomas oligodendroglioma, IDH-mutant and 1p/19q co-deleted; Astrocytoma, IDH-mutant (non-co-deleted); and Glioblastoma (GBM), IDH-Wildtype (WT) [4]. The subsequent WHO 2024 update further emphasized the prognostic significance of the IDH status. Under the current criteria, IDH-Wildtype Astrocytoma are no longer considered low-grade lesions but rather represent early Glioblastoma stages, leading to their reclassification as Glioblastoma (GBM). Crucially, the absence of an IDH mutation is the defining characteristic of primary Glioblastoma (CNS WHO Grade 4). IDH-wildtype neoplasms that possess the molecular features of Glioblastoma consistently have poorer outcomes compared to IDH-mutant gliomas of the same histological grade. This molecular reclassification underscores that the absence of an IDH mutation is sufficient to classify a high-risk, Grade 4 equivalent disease. Consequently, the GBM, IDH-Wildtype cohort represents the most aggressive and prognostically challenging subtype under current diagnostic standards [5].

Unfortunately, currently the average survival rate of patients with GBM live is about 14–15 months with the available therapies which include surgical resection followed by simultaneous radiotherapy and temozolomide (TMZ)-based chemotherapy [6]. Therefore, there is an urgent need to better understand molecular underpinnings of GBM for identification of novel molecular targets and development of more effective treatments [7, 8].

Recent research highlights the crucial role of microRNAs (miRNAs) in the development of various malignant tumors, including glioblastoma (GBM) [9, 10]. A growing body of evidence indicates that numerous miRNAs are expressed aberrantly in human cancers [11–13].

Among these, the expression of miR-484 varies significantly across different tumor types. It has been shown to be downregulated in cancers such as gastric cancer [14, 15], pancreatic cancer [16], and estrogen receptor-positive breast cancer [17]. Conversely, miR-484 is upregulated in other cancers, including prostate cancer [18], non-small-cell lung cancer (NSCLC) [19], hepatocellular carcinoma [20], and some forms of breast cancer [21].

The function of miR-484 in GBM remains unclear. Two studies on glioma have presented conflicting results: they indicate that its upregulation is negatively correlated with patient survival and that it is associated with tumor progression [22, 23]. Based on this conflicting data, it is not yet certain whether miR-484 acts as a tumor suppressor or an oncogene in IDH1 mutated and WT tumors.

Therefore, we aimed to evaluate its significance in IDH1-mutated and wild-type (WT) tumors.

Forkhead Box M1 (FOXM1), which is an oncogenic transcription factor, expression is correlated with a malignant phenotype and poor prognosis in GBM [23–26]. miR-484 has physiological functions in both cancer and non-cancerous diseases, including roles in endoplasmic reticulum stress, oxidative stress, inflammation, cell proliferation, and apoptosis [27]. Therefore, we also hypothesized a relationship between FOXM1 and miRNA-484 considering the functions of miR-484 and FOXM1 in GBM cells. Then, we performed target analysis using the miRWalk tool (http://mirwalk.umm.uni-heidelberg.de/human/interaction/21414864/), in silico data showed a stable and specific binding between miR-484 and FOXM1 (binding energy = -25.4 kcal/mol) (Fig. 6d). Subsequently, we aimed to investigate role and molecular mechanisms of miR-484-induced effects in GBM cells. Our findings suggest that IDH1-wild type patients had lower miR-484 expression patterns than IDH-mutant patients, and miR-484 expression suppressed cell proliferation, colony formation, migration, and induced apoptosis by targeting FOXM1 oncogenic signaling in GBM cells. Also, we found that expression of miR-484 suppressed expression of FOXM1 and its downstream target proteins (Integrin-β1/FAK/Src and Cyclin-D) and DNA repair enzyme PARP in GBM cells. Moreover, the presented study demonstrated that miR-484 enhanced the therapeutic effect of TMZ-in GM cells. Overall, our present work provides the first evidence that miR-484 functions as a tumor suppressor in GBM cells by inhibiting FOXM1 expression. Collectively, our findings may provide insights into the role of miR-484 in high grade GBM cells, and response to TMZ in GBM cells, miR-484-based therapeutic strategy may be considerable against GBM.

Table 1 Patients' characteristics and clinicopathological features

Cohort	Treatment naïve primary glioma patients
Patient number	29
Mean (range) age at diagnosis	51.59 ± 11.34 (28–72)
Gender	
Male	14
Female	15
Histologic grade	
II	5
III	1
IV	22
IDH1 mutation status	
Mutant (IDH1 R132H)	10
Wild type	19

Materials and methods

Patients and specimens

Fresh tissue samples were collected from 29 patients (IDH wild type (n = 19), IDH mutant (n = 10)) confirmed with neuropathologically newly diagnosed and treatment-naïve brain tumors (WHO grades II-IV) at Erciyes University Medical Faculty Hospital. All the patients gave written informed consent, and the Clinical Research Ethics Committee of Erinyes University approved this investigation (decision no: 2019/247). The characteristics and clinicopathological features of all patients were summary in Table 1. Other details on all of the patients were listed in supplementary information (Table S1).

Cell lines and culture conditions

We used human IDH1-wild type U87-MG (cat# HTB-14) and IDH1-mutant-U87 (cat# HTB-14IG) cell lines, which were purchased from the American Type Culture Collection (Manassas, VA, USA). These cells were cultured in Dulbecco's Modified Eagle's Medium (DMEM)/F12, which was supplemented with 10% fetal bovine serum (Sigma-Aldrich, St. Louis, MO) [28].

Transfection with miRNAs and siRNAs

The hsa-miR-484-mimics (MC10379, Cat# 4,464,067, Ambion), hsa-miR-484-inhibitor (MH10379, Cat# 4,464,085, Ambion), and control miRNAs, which are miRNA sequences designed not to target any known genes and serve as negative controls to assess the non-specific effects of miRNA transfection, were obtained from Thermo Fisher Scientific. Actively growing U87-MG and IDH1-mutant-U87 GBM cells were plated 24 h before transfection and transfected with either miR-484 mimics or inhibitors (mature miR-484 sequence: UC AGGCUCAGUCCCCUCCCGAU), and NC miRNA at a final concentration of 50 NM for 72 h, using HI Perfect Transfection Reagent (Qiagen, Valencia, CA) according to the manufacturer's protocol [27, 29–33]. Two different small interfering RNAs (FOXM1#1 siRNA, Cat# SASI_Hs01_00052108; FOXM1#2 siRNA, Cat# SASI_Hs01_00243977) targeting FOXM1 gene and non-silencing control siRNA (Cat# WD00909801) were purchased from Sigma-Aldrich [28–31]. Following treatment, the cells were harvested and processed for further analysis.

Cell viability and colony formation assays

We analyzed the viability of U87-MG and IDH1-mutant-U87 GBM cells using an MTS assay, as previously described [29, 30, 35]. The cells were seeded in 96-well plates at a density of 1.2×10^5 cells /well. After an overnight incubation, the cells were transfected with miRNAs at a final concentration of 50 nM for 72 h.

Following the transfection, a solution of MTS and phenazine methosulfate (20:1 v/v) was added to the cells.

After a 3-h incubation at 37 °C, we measured the number of viable cells by reading the absorbance at 490 nm using a plate reader. This measurement is based on the formazan produced by the viable cells.

Clonogenic assays were performed to assess colony formation in U87-MG and IDH1-mutant-U87 GBM cells. Cells were seeded in six-well plates at a density of 1.5×10^3 cells/well. Three sets of experiments were conducted. For the first set, cells were transfected with miR-484 mimic, inhibitor, or control-miR (50 nM) for 72 h. Colony formation was then enabled to proceed until visible colonies appeared, as previously described [28–31]. In the second set, U87-MG and IDH1-mutant-U87 GBM cells were transfected with control siRNA and FOXM1 siRNAs (50 nM) for 48 h and subsequently grown for 2 weeks. The third experiment involved treating U87-MG cells with increasing doses of TMZ (10, 25, 50, and 100 μM). Additional treatment groups included DMSO alone, miR-484 mimic (50 nM) alone, control-miR alone, and a combination of TMZ (10 μM) with miR-484 mimic (50 nM). Colony formation was allowed to proceed until visible colonies appeared. Following colony formation, we washed the cells with PBS and stained them with crystal violet. For the quantification of colonies, size-based exclusion criteria were using ImageJ software. To ensure the exclusion of satellite colonies, an automated area threshold of 450 to 1900 pixels was applied. Then, through manual cell-by-cell was counted of at 450-pixel threshold colonies using the Leica Application Suite, and our results showed that an area of 450 pixels corresponds to more than 50 cells (Fig.S1), by the standard criterion that a colony must consist of at least 50 cells. All experiments were conducted in triplicate [28–31].

Wound-healing assay

U87-MG and IDH1-mutant-U87 GBM cells were plated in six-well plates (1.5×10^5 cells/well). After 24 h of incubation, cells were transfected with miR-484 mimic and inhibitor or control miRNA. After 72 h, the surface of the cell layer was carefully scratched using a 20-μl sterile tip and cellular debris was removed by washing with medium, then fresh medium was added to the cells. The cells were photographed right away (time point, 0 h) using a phase-contrast microscope (Leica) to determine the wound width. The cells were photographed again at 24 time points. The photographs were compared, and the distance traveled by cells at the leading edge of the wound at each time point was measured. The results were expressed as an average distance between the edges of the gap. All experiments were done in triplicate [28–31].

Invasion assay

We transfected U87-MG and IDH1-mutant-U87 GBM cells with either miR-484 mimics, inhibitors, or a control miRNA. After 72 h, we seeded equal numbers of viable transfected cells (5×10^4 cells/well) onto Matrigel-coated Transwell filters (8-mm-pore-size) in Matrigel Invasion Chambers. We then counted the number of cells that had invaded the lower side of the membrane after 24 h by counting cells in at least four random fields [31].

Western blot analysis

U87-MG and IDH1-mutant-U87 GBM cells (3.5×10^5) were seeded in T-25 flasks. After 24 h, they were transfected with miRNAs (50 nM) for 72 h. The cells were then collected, washed twice with ice-cold PBS, and lysed in a lysis buffer at 4 °C.Protein concentrations were measured using a protein assay kit (DC kit; Bio-Rad). A total of 40 μg of protein from each sample was separated by 4–20% SDS–polyacrylamide gel electrophoresis and transferred to polyvinylidenedifluoride membranes. The membranes were then blocked for 60 min with a blocking buffer (0.1 Triton X-100 with 5% dry milk in TBS-T). After washing with TBS-T, the membranes were probed with the following primary antibodies: FOXM1 (Cell signaling, cat# 5436S), Integrin-β1 (Proteintech, cat# 12,594–1-Ap), p-Src (Cell signaling, cat# 12432S), Src (Proteintech, cat# 11,097–1-Ap), p-FAK (Cell signaling, cat# 8556S), FAK (Proteintech, cat# 12,636–1-Ap), PARP (Proteintech, cat# 13,371–1-Ap), cyclin-D1 (Proteintech, cat# 55,004–1-Ap) and β-actin (Proteintech, cat# 60,008–1-Ig). After being washed with TBS-T, the membranes were incubated with horseradish peroxidase-conjugated anti-rabbit (Bio-Rad, #170–6515) or anti-mouse secondary antibody (Bio-Rad). β-actin was used as a loading control. All antibodies were diluted in 1xTBS-T containing 5% dry milk (dilution rate was 1:1000 for antibody to TBS-T). We used Clarity Western ECL Substrate (Bio-Rad) for chemiluminescence detection. The blots were then visualized and quantified with a densitometer using a ChemiDoc MP Imaging System (Bio-Rad) and its corresponding application program [28–31].

Detection of apoptotic cell death

U87-MG and IDH1-mutant-U87 GBM cells were seeded in 96-well plates (1×10^4cells/well) and 24 h later were transfected with miRNAs (50 nM) for 72 h. Furthermore, cells were seeded in 96-well plates (1×10^4cells/well) and treated with TMZ (40 μM) and DMSO as controls for 72 after incubation, the supernatant was removed, and cells were blocked with Fc-block for 5 min on ice. The cells were then stained using BioLegend's FITC Annexin V Apoptosis Detection Kit with 7-AAD (cat#640,922) and analyzed via FACSARIAIII (Becton Dickinson) [32].

Cell cycle analysis

For cell cycle analysis, U87-MG GBM cells were seeded into 6-well plates at a density of 200,000 cells/well. The

cells were transfected with miRNAs (50 nM) or treated with TMZ (40 μM) and DMSO controls for 72 h. After harvesting, the cells were fixed overnight at -20 °C in 70% EtOH.

Fixed cells were then washed with PBS by centrifugation. They were treated with RNase (500 U/mL) for 30 min at 37 °C, followed by centrifugation to remove the supernatant. The cell pellet was stained with propidium iodide (PI) and incubated for 30 min. Finally, a Guava Easy Cyte flow cytometer was used to perform the analysis with a red fluorescence filter [33].

RNA extraction and qRT-PCR analysis

Total RNA was extracted from patient cancer tissues and from transfected U87-MG and IDH1-mutant-U87 GBM cells. The transfections were performed with miR-484 mimics/inhibitors or FOXM1-siRNAs/control siRNA, using the manufacturer's protocol (Roche, High Pure RNA isolation kit). Subsequently, 1 μg of RNA from each sample was reverse transcribed in triplicate using the MicroRNA reverse transcription kit (Takara Bio USA, Inc, cat#638,313). The qPCR reaction was then carried out using TB green real time PCR Premix to amplify U6 snRNA (endogenous control) and the target hsa-miR-484. All reactions were run in triplicate on a Light cycler 480 Real-Time PCR System. For relative quantification, all data were normalized to the geometric average of all samples. Differences in expression were calculated using the delta-delta Ct (ddCq) method, and fold change was determined using the formula 2ddCq [30].

Bioinformatics analysis

We performed Gene Ontology (GO) and Kyoto Encyclopedia of Genes and Genomes (KEGG) pathway enrichment analyses to identify the molecular pathways of miR-484. This was done using DIANA-miRPath v3.0 (http://www.microrna.gr/miRPathv3)., with a significance cutoff of $p < 0.05$. We also analyzed the expression profile of miR-484 in cancer using the cBioPortal for Cancer Genomics, a tool that visualizes and analyzes large-scale cancer genomics datasets(https://www.cbioportal.org/). Additionally, we used TransmiR v2.0 to investigate the regulatory relationship between FOXM1 and miR-484 ((http://www.cuilab.cn/transmir) [30]. To investigate the potential regulatory relationship between miR-484 and the transcription factor FOXM1, we first predicted their specific binding using the miRWalk tool (http://mirwalk.umm.uniheidelberg.de/human/interaction/21414864/). Subsequently, we performed comprehensive analysis using data from The Cancer Genome Atlas (TCGA) to assess the prognostic relevance of FOXM1 expression levels across relevant cancer cohorts (https://ualcan.path.uab.edu/cgi-bin/TCGA-survival1.pl?genenam=FOXM1&ctype=GBM).

RNA-seq analysis

The miR-484 mimic and control miRNA was transfected into U87-MG and IDH1-mutant-U87 GBM cells in a six-well plate for 72 h, and total RNA was extracted using TRIzol Reagent (Roche, High Pure RNA isolation kit, Germany)) according to the manufacturer's instructions. Total RNA was sent to RefGen BIOTECHNOLOGY LTD (https://www.refgen.com/Ankara, Turkey) for quality control, purification, screening, and transcriptome sequencing. Gene Set Enrichment Analysis (GSEA), Kyoto Encyclopaedia of Genes and Genomes (KEGG) pathway, and Gene Ontology (GO) analyses were used to analyse and present the results of RNA-seq ($p < 0.05$, for statistical significance). For quality control of isolated RNA material, quantity, purity, and structural integrity were determined using fluorometric and capillary electrophoresis methods. Measurements were performed using a Qubit 3 fluorometer (Thermo Fisher, USA, #Q33216) and either a 2100 Bioanalyzer (Agilent, USA, #G2939BA) or, alternatively, a 4200 TapeStation (Agilent, USA, #G2991BA). For library preparation of the isolated RNA material, the Illumina Total RNA Prep kit (Illumina, USA, #20,040,529) was utilized. The sequencing was performed on an Illumina NovaSeq 6000 next-generation sequencing platform. After the sequencing process, the FASTQC tool was used for quality control of the obtained read data. For trimming based on quality scores, the Trimmomatic (v0.39) tool was used. After trimming, the resulting sequences were analyzed using the Illumina DRAGEN Bio-IT platform and its RNA Pipeline workflow. During this analysis, reads were splice-aware aligned to the chosen genome. The current reference genome for the relevant organism (Homo Sapiens GRCh38.p13) was used as the reference. For annotation after alignment, the GENCODE 40 dataset was used for gene, exon, and transcript information. Following this process, read counts on each transcript were calculated and then normalized by the transcript's length to obtain RPK (Reads per Kilobase) values. These values were then re-normalized by the total read count to derive TPM (Transcripts Per Million) values. After normalization, the edgeR R package and the Quasi-Likelihood model were used to identify Differentially Expressed Genes between groups. Gene ontology analysis employed the TopGO package and the Kolmogorov–Smirnov (KS) statistical test. For pathway analyses, the clusterProfiler package was utilized. Finally, R scripts were used for organizing intra-group and inter-group statistical comparisons, data visualization applications, and report generation.

Statistical analysis

Results were summarized as the mean ± standard deviation. We used the Student's t-test to determine statistical significance, with a p-value of less than 0.05 considered

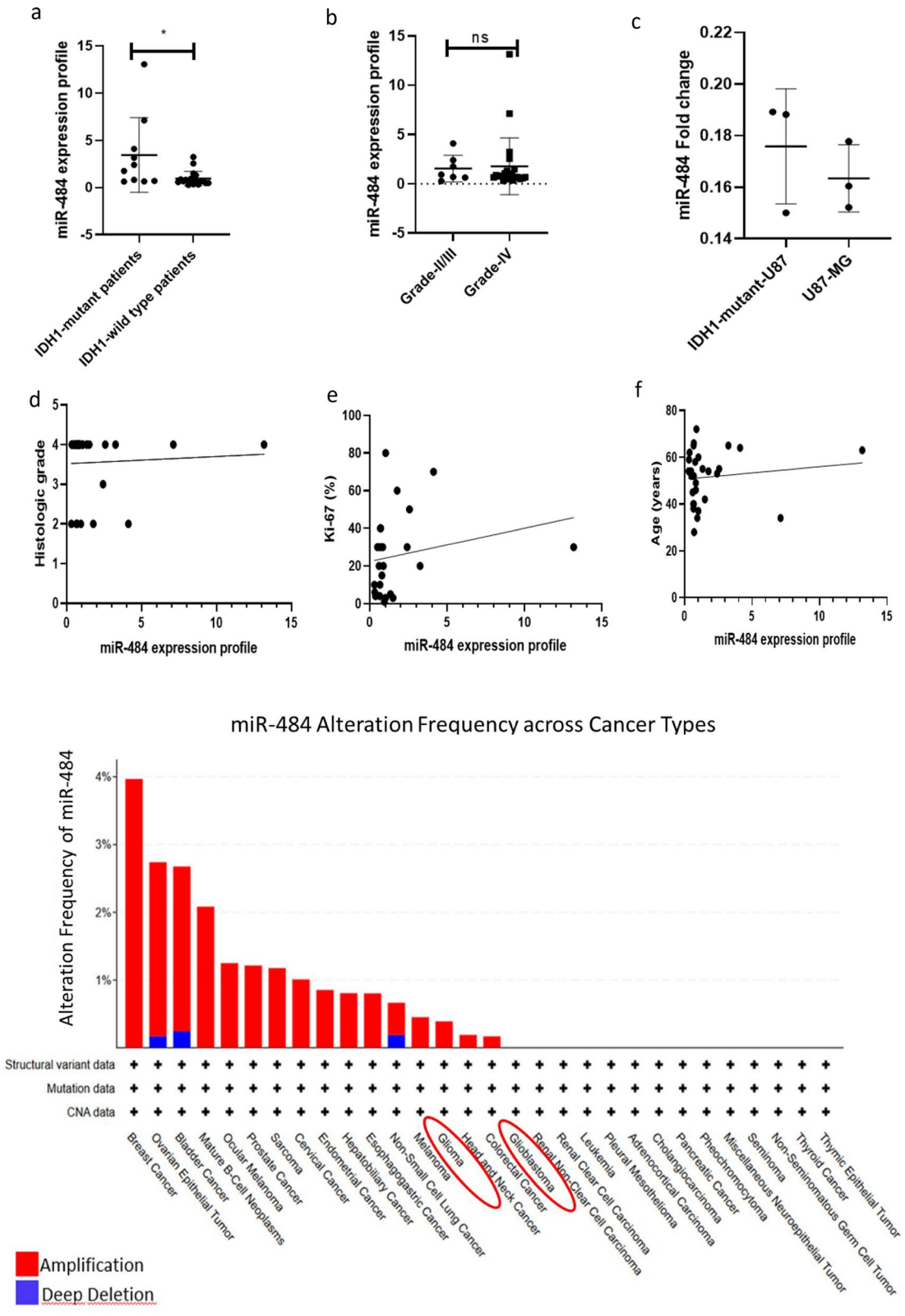

Fig. 1 (See legend on next page.)

(See figure on previous page.)

Fig. 1 Expression of miR-484 in IDH-wild type and IDH-mutant GBM tumor tissues and cell lines**.** (**a**) The relative levels of miR-484 in IDH-wild type and matched IDH-mutant GBM tumor tissue were evaluated using RT-PCR. (**b**) Correlation of miR-484 expression with histologic grade. (**c**) miR-484 expression in IDH-wild type and IDH-mutant GBM cells. (**d**), Ki-67(**e**), ages (**f**) of patients. (**g**) Genetic alteration frequency of miR-484 across the was plotted using database cBioPortal for Cancer Genomics providing visualization and analysis large-scale cancer genomics data sets (https://www.cbioportal.org/). Alterations are categorized as Amplification (red bars) and Deep Deletion (blue bars). The alteration frequency in Brain Lower Grade Glioma (LLG) and Glioblastoma Multiforme (GBM) amplifications predominant (*$P < 0.05$, ns, not significant)

significant. We also performed a Pearson's correlation analysis to evaluate the association between histologic grades, Ki-67, and miR-484 fold-change. The discriminatory power of miR-484 was evaluated through Receiver Operating Characteristic (ROC) analysis to determine its potential as a diagnostic or prognostic biomarker. All data were analyzed and graphed using GraphPad Prism 8.

Results

Tissues of IDH-mutant and IDH-wild type patients exhibit different miR-484 expression profile.

IDH-mutant patients (IDH1 (+)) have a better prognosis and longer survival compared to IDH wild type patients (IDH1 (-)). Therefore, we investigated whether the expression profile of miR-484 plays a role in this difference between IDH (+) and IDH (-) patients by performing quantitative RT-PCR. We observed distinct miR-484 expression profiles in tissues from IDH- (+) (n = 10) and IDH-(-) (n = 19) patients (Fig 1a).

miR-484 levels were significantly lower in the tissues of IDH-(-) patients compared to those of IDH-(+) patients (Fig 1a and Table 2). We further examined miR-484 expression across different malignancy grades. Patients classified as Grade II/III and Grade IV exhibited similar overall miR-484 expression profiles, although patients with low-grade gliomas had a slightly higher miR-484 expression level compared to patients with high-grade disease (Fig 1b).

In in vitro models, while no significant difference was detected between U87-MG cells and IDH1-mutant-U87 GBM cells, IDH wild-type U87-MG cells showed a relatively lower expression level when compared to IDH1-mutant-U87 GBM cells (Fig 1c).

Next, we investigated the relationship between the miR-484 expression profile and various clinicopathological features. We found no significant association between miR-484 expression and histological grades (Fig 1d), proliferation marker Ki-67 values (Fig 1e), or patient age (Fig 1f).

The visualization and analysis features of the cBioPortal support studying different types of gene alterations in tumors simultaneously [34]. Therefore, we utilized the cBioPortal for Cancer Genomics database [34]. As demonstrated in Fig. 1g which plots the genetic alteration frequency of miR-484 across various cancer studies within The Cancer Genome Atlas (TCGA) PanCancer Atlas, distinct patterns were observed in central nervous system malignancies. Specifically, the alteration frequency of miR-484 was approximately 1.1% in Brain Lower Grade Glioma (LLG). In contrast, GBM exhibited a lower frequency (approximately 0.5%). Crucially, for both tumor types, the observed alterations were predominantly amplifications of miR-484, visually represented by the red bars. Subsequently, to experimentally validate these database findings, we assessed miR-484 expression in tumor tissue samples from IDH-wild type and IDH-mutant patients using qRT-PCR. Our results demonstrated that miR-484 expression was markedly lower in tumor tissue from IDH-wild type patients compared to that of IDH-mutant patient tumor tissue, which aligns with lower-grade glioma characteristics [4]. These patient data confirmed the miR-484 expression patterns predicted by the cBioPortal database (Fig 1g).

Diagnostic and prognostic potential of miR-484

Given the observed differential expression, the potential of miR-484 to discriminate between clinical groups was assessed. Receiver Operating Characteristic (ROC) curve analysis was performed to evaluate the diagnostic power of miR-484 expression for distinguishing between IDH-mutant and IDH-wild type patients (Fig 2a). The highly favorable position of the curve suggests a strong discriminatory power (AUC = *0.7860, P* < 0.01). Our analysis provides that miR-484 expression possesses strong prognostic potential to differentiate between these two key molecular subgroups.

The prognostic value of the FOXM1 was assessed using Kaplan–Meier survival analysis in TCGA cohorts. In GBM patients (n = 113), high expression of FOXM1 was associated with poorer overall survival compared to patients with low/medium expression, although this difference did not reach statistical significance (Fig 2b, P > 0.05). These survival analyses, despite lacking strong statistical significance in the TCGA cohorts, suggest FOXM1 acts as a negative regulator of the tumor-suppressive miR-484, contributing to the aggressive phenotype in GBM.

miR-484 expression suppressed colony formation, migration and invasion and induces apoptosis in IDH-wild type and IDH1-mutant- GBM cells

To evaluate the functional role of miR-484 in two different GBM cells U87-MG and IDH1-mutant-U87 GBM cells were transfected with mimic-miR-484 or

Table 2. miR-484 expression profile of patients

Chort	n	miR-484 expression profile Mean ± SD
Histologic Grade-II/III	6	1.125 ± 0.7983
Histologic Grade-IV	19	0.9793 ± 0.7271
IDH (-)	19	0.9646 ± 0.1742
IDH (+)	10	3.244 ± 4.049

SD: Standart devation.

inhibitor-miR-484. Firstly, in transfected U87-MG and IDH1-mutant-U87 GBM cells with mimic-miR-484 and inhibitor-miR-484 or control miRNA, transfection efficiency was determined by Real-time PCR. As shown in Fig. 3a-b, mimic-miR-484 increased the expression of miR-484, and it was downregulated in the presence of inhibitor-miR-484, indicating that the cells were successfully transfected with miR-484 mimic or inhibitor (Fig 3 a-b). Next, we evaluated cell proliferation and colony formation by MTS and clonogenic assays. The MTS analysis revealed that mimic-miR-484 significantly reduced cell proliferation of U87-MG and IDH1-mutant-U87 GBM cells compared to transfected cells with inhibitor-miR-484 and control cells (Fig. S2 a, b). mimic-miR-484 suppressed the colony number in U87-MG and IDH1-mutant-U87, while inhibitor-miR-484 did not affect cell proliferation compared with control-miR-transfected cells (Fig 3 c-d).

Next, to assess whether miR-484 is involved in motility and migration of U87-MG and IDH1-mutant-U87 cells, we performed an in vitro wound healing assay. Cells were transfected with mimic-miR484, ınhibitor-miR-484 or control-miR. 72 h after transfections, a single scratch wound was created in the well, and the cells were monitored for 24 h. As shown in Fig 3 e–f, while in cells transfected with control mir-484 or inhibitor-miR484 the wounded areas were completely closed by migration of cells, the expression of miR- 484 by mimic mir-484 decreased migration of cells, indicating that in cells with miR-484 expression were suppresses to migrate or mobility (Fig 3 e–f).

Next, In vitro matrigel invasion assay demonstrated that mimic miR-484 impaired the invasiveness of U87-MG and IDH1-mutant-U87 cells compared to control miRNA-transfected cells, as indicated by less number of cells invading the bottom part of the well. Whereas inhibitor-miR-484 did not alter the invasiveness of U87-MG and IDH1-mutant-U87 cells, indicating miR-484 suppresses cell invasiveness (Fig 3 g-h).

miR-484 expression suppresses FOXM1 oncogenic signaling in GBM cells

FOXM1 is an oncogenic transcription factor that is unregulated in GBM [23–26]. In our previous studies, we demonstrated that FOXM1 is highly expressed in GBM cells and drives cell proliferation, colony formation and migration/invasion and inhibits apoptosis in GBM cells [27]. In the current study, we also demonstrated that knockdown of FOXM1 by two different FOXM1siRNAs completely inhibits cell proliferation and colony formation in IDH wild type U87-MG cells

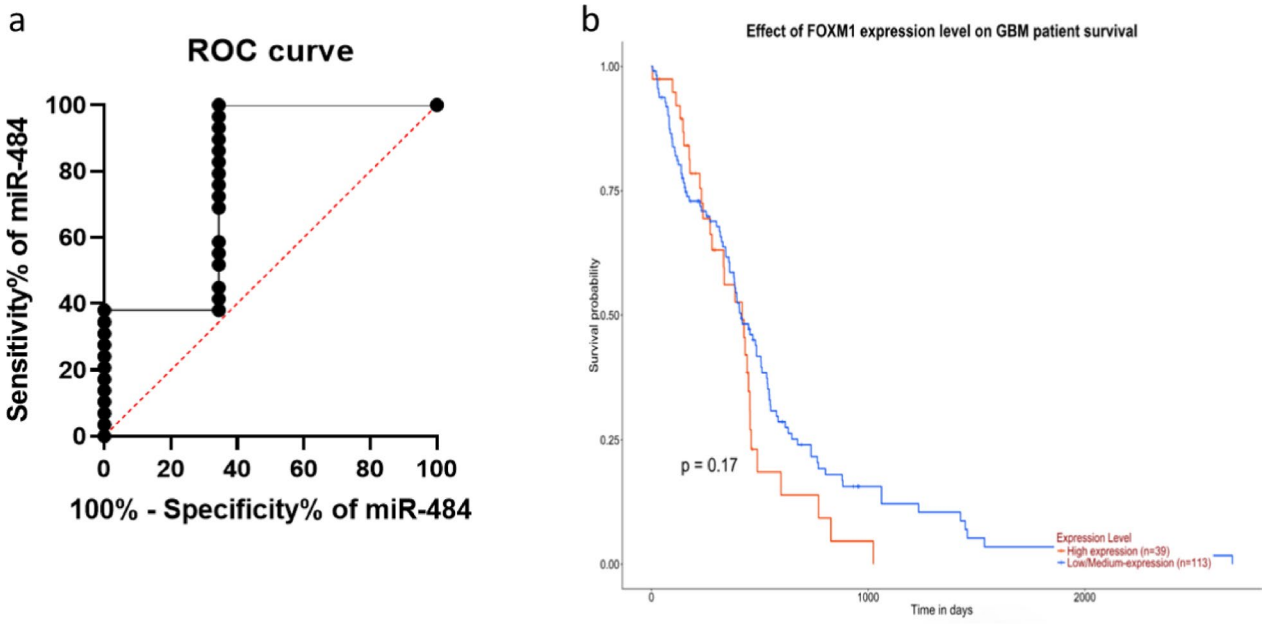

Fig. 2 Prognostic/diagnostic value of miR-484 and effect of FOXM1 and mir-484 expression on glioma patient survival. (**a**) ROC curve analysis for evaluating the prognostic/diagnostic value of miR-484 in IDH-wild type and IDH-mutant glioma (AUC = 0.7860, $P < 0.01$). (**b**) Kaplan–Meier survival analysis comparing overall survival in GBM patients with high expression of FOXM1 (n = 39) versus those with low expression (n = 113)

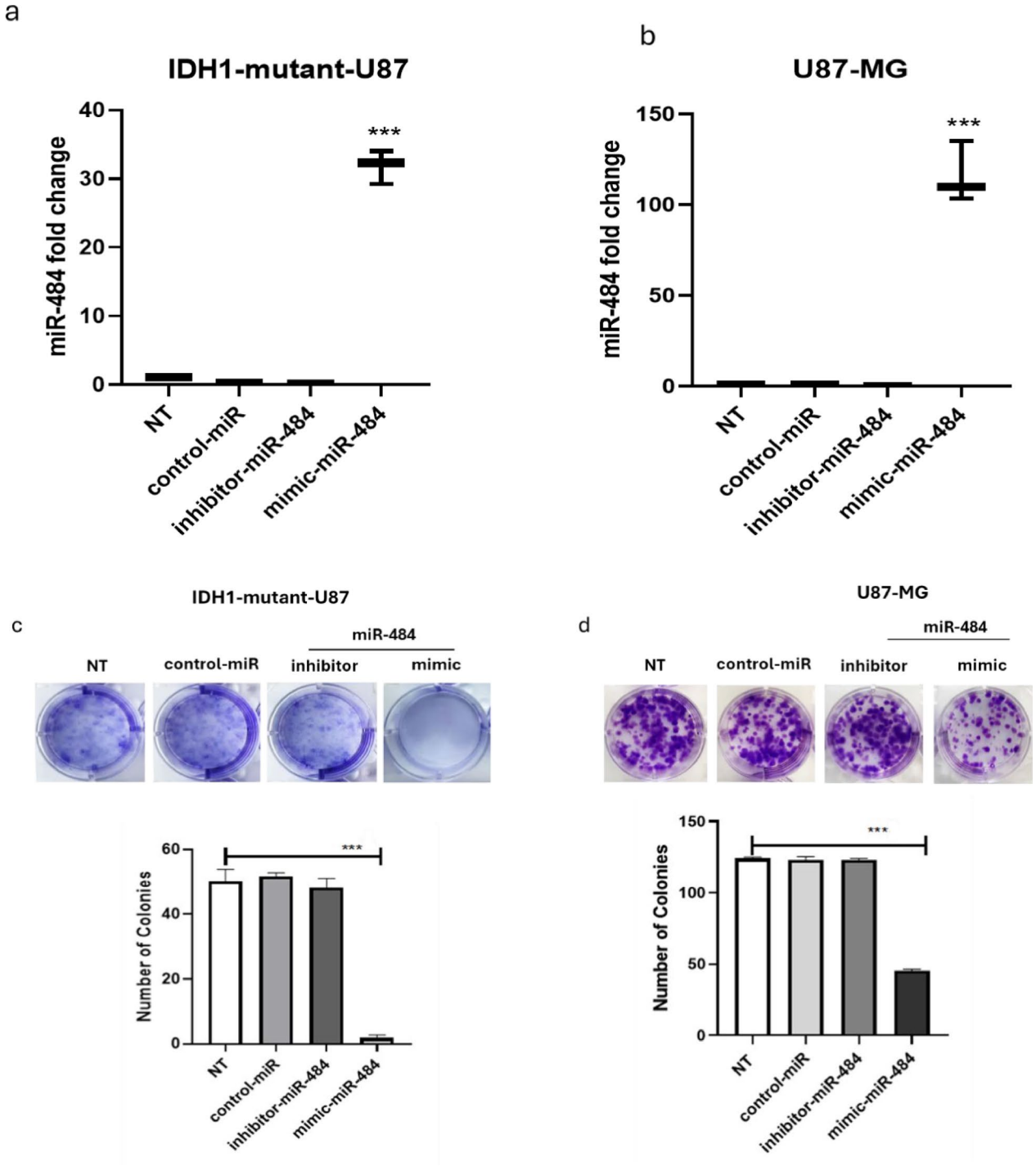

Fig. 3 miR-484 expression suppresses colony formation, migration and invasion of GBM cells. (**a-b**) miR-484 expression after mimic-miR-484 and inhibitor-miR-484 transfections in GBM cells detected by (RT-PCR). (**c-d**) After mimic-miR-484 and inhibitor-miR-484 transfections and colonies were counted at day 14. (**e–f**) GBM cells were transfected with miRNAs and cell migration was measured by a wound healing assay. The bar graph shows the number of witdh of the wound. (**g-h**) GBM cells were transfected with control or miRNA-484 (for 72 h), and equal numbers of viable cells were seeded onto Matrigel-coated Trans well filters in Matrigel invasion chambers. The number of the cells that invaded matrigel and passed through membrane were photographed and counted after 24 h. The bar graph shows the mean of percentages of cells invaded the matrigel. The data were presented as means with standard deviations (± SD) of three experiments (**$P < 0.01$ and ***$P < 0.001$)

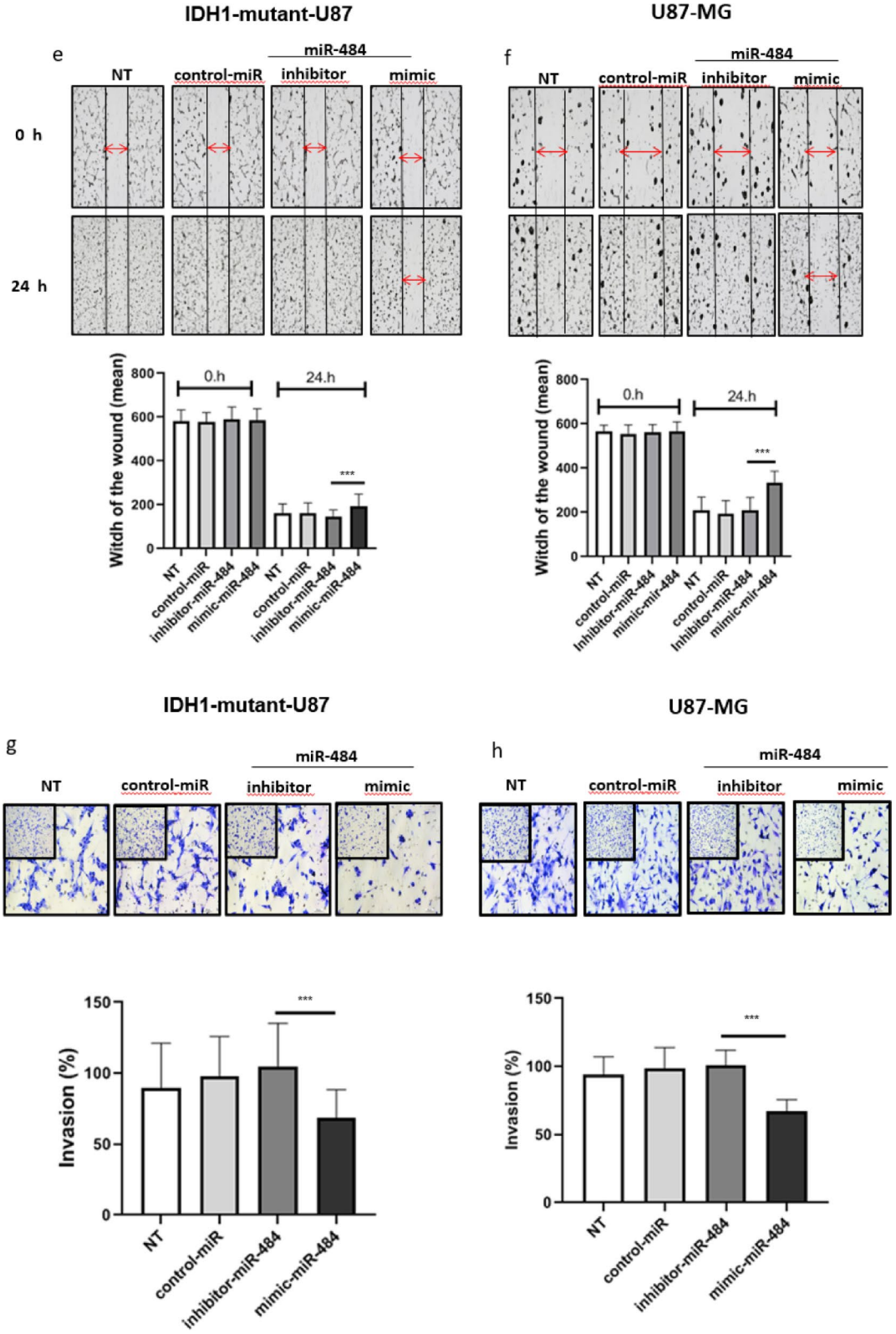

Fig. 3 (continued)

and IDH1-mutant-U87 cells compared to control-siRNA treated cells (Fig 4, a-b). Next, we evaluated expression of FOXM1 and its downstream targets in transfected IDH1-mutant-U87 cells and U87-MG with mimic-miR-484 or

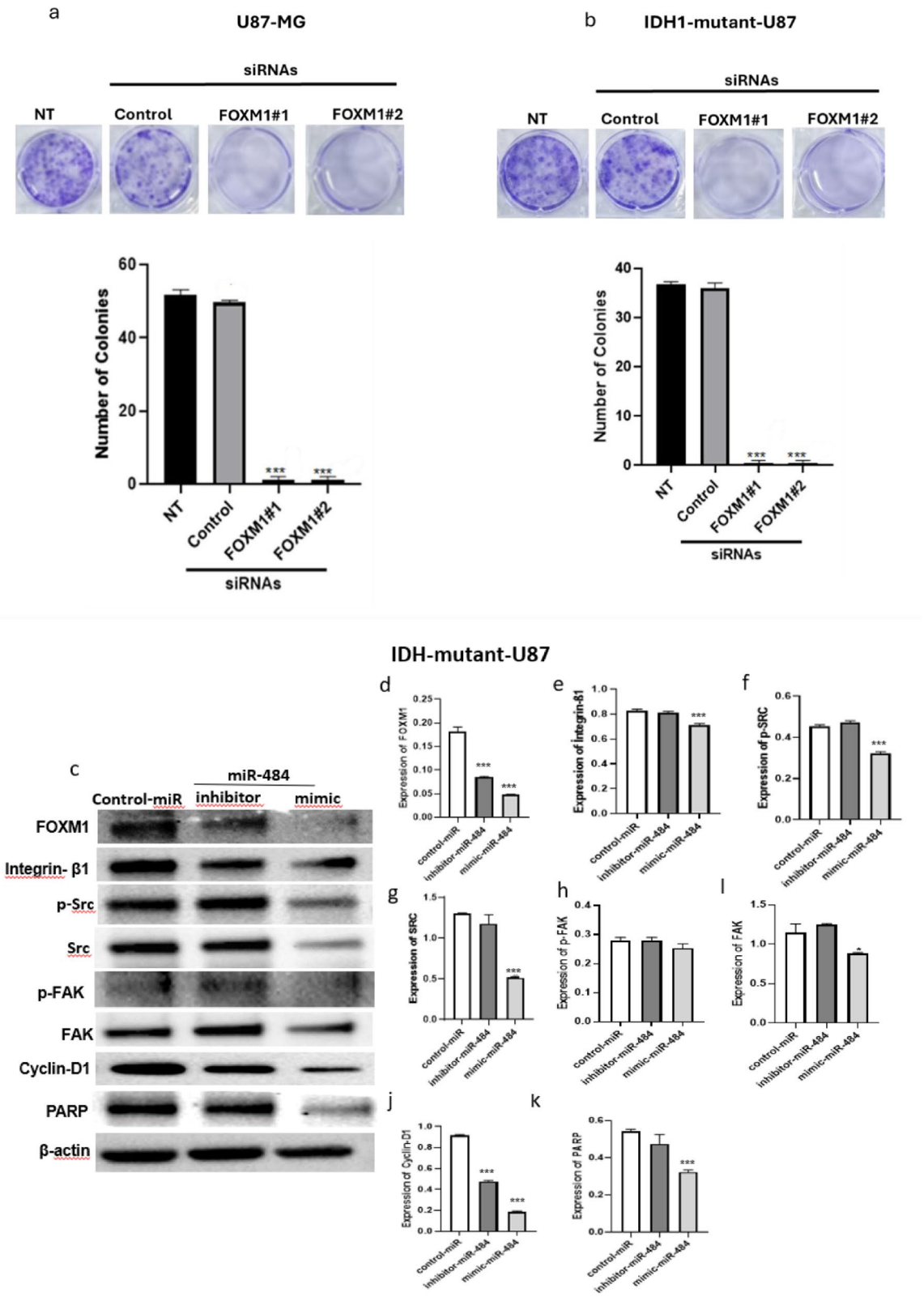

Fig. 4 miR-484 suppresses expression of FOXM1 and its downstream targets, Integrin-β1, Src, FAK and Cyclin-D, and DNA repair enzyme PARP in GBM cells. (**a-b**) Cells were transfected with two different FOXM1 siRNAs and control siRNA. The colonies (areas) were measured by image J at the end of the 14 days. (**c-u**) U87-MG and IDH1-mutant-U87 cells were transfected with control-miR or miRNA-484 mimic. Protein extracts were isolated 72 h after transfection. Expression of miR-484 inhibits expression levels of FOXM1 and its downstream targets and PARP. β-actin was used as a loading control. Band intensities were evaluated by densitometric analysis. (*$P < 0.05$, **$P < 0.01$, *** $P < 0.001$, ns, not significant)

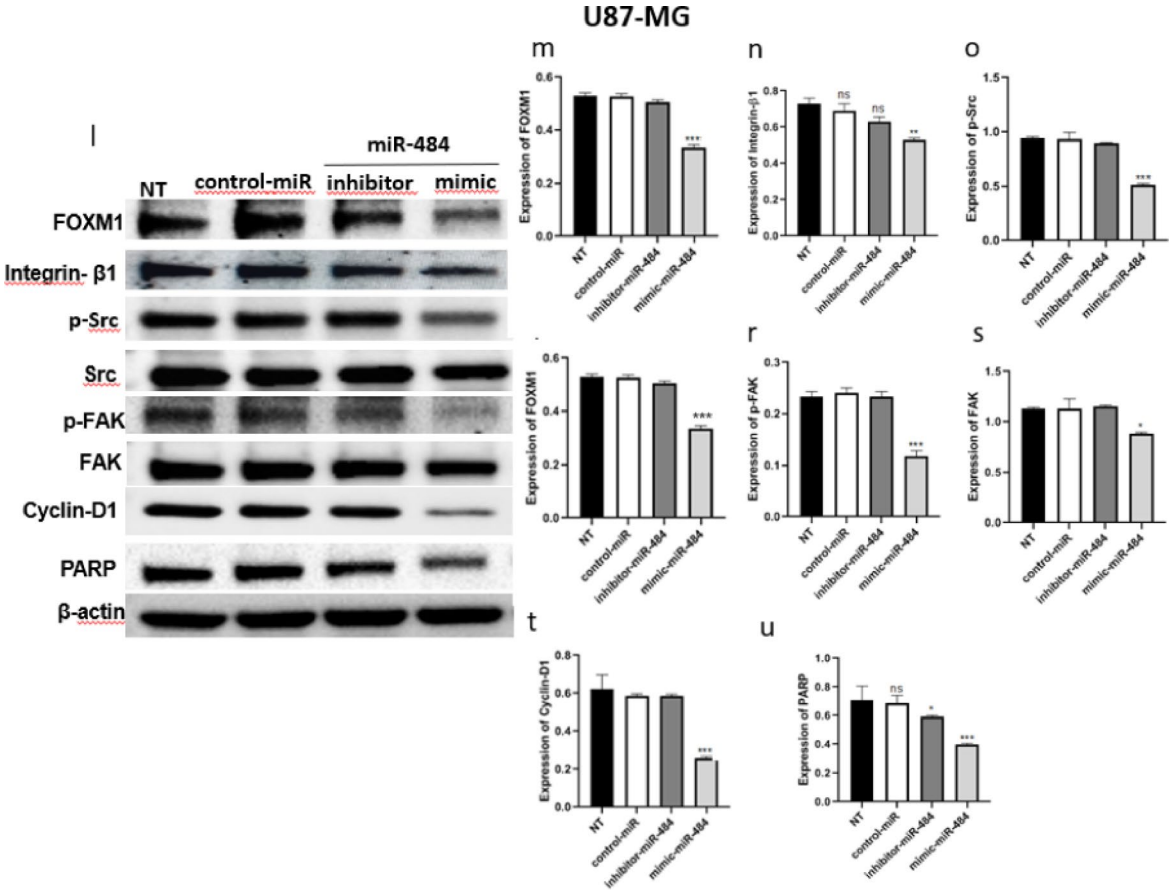

Fig. 4 (continued)

inhibitor-miR-484 by western blot analysis. As expected, we found that miR-484 expression by mimic-mir-484 decreased expression of FOXM1 and its downstream targets including integrin β1(which is essential for cell migration and invasion) and Cylin-D1 (which promotes the cell cycle by inducing G1 phase) and reduced phosphorylation of Src and FAK (which are most important mediators of cell migration/invasion) (Fig 4 c-k, l-u). Also, expression of miR-484 led to decreased expression of total PARP1 protein (which plays roles in DNA repair) (Fig 4 c, k, 1, u).

Partial differences in protein expression were found between U87-MG and IDH1-mutant-U87 GBM cells after transfection with miR-484 mimic and inhibitor. We believe that these partial differences may be associated with metabolic consequences derived from IDH mutations.

Our findings indicated that miR-484 act as a tumor suppressor and suppresses cell proliferation, migration and invasion by inhibition of FOXM1 expression and its downstream mediators including Integrin-β1/SRC/Fak/cyclin-D axis in GBM cells.

miR-484 mimic treatment sensitizes wild-type-GBM to temozolomide

FOXM1 activates expression of DNA repair proteins that is linked TMZ resistance in glioma cells [36]. Because miR-484 expression led to a decrease in FOXM1 expression we hypothesized that miR-484 expression may sensitize cells to TMZ and investigated whether mimic-miR-484 treatment increases effect of TMZ in GBM cells. Based on our hypothesis that miR-484 expression may sensitize GBM cells to TMZ by downregulating FOXM1, a protein linked to TMZ resistance, we investigated the effect of miR-484 mimic-based therapy, both alone and in combination with TMZ, on cell colony formation, apoptosis, and FOXM1's downstream targets. The cell proliferation/viability (MTS) and colony formation analysis revealed that treatment of cells with TMZ resulted in a dose-dependent manner inhibition of cell proliferation compared to control cells. (Fig. S3). After finding IC25 doses of TMZ (10 μM) in cell proliferation/viability and colony formation, we investigated the combined effects mimic-miR-484 and TMZ treatment on colony formation of U87-MG cells. Our results demonstrated that the combination of mimic-miR-484 and TMZ suppressed

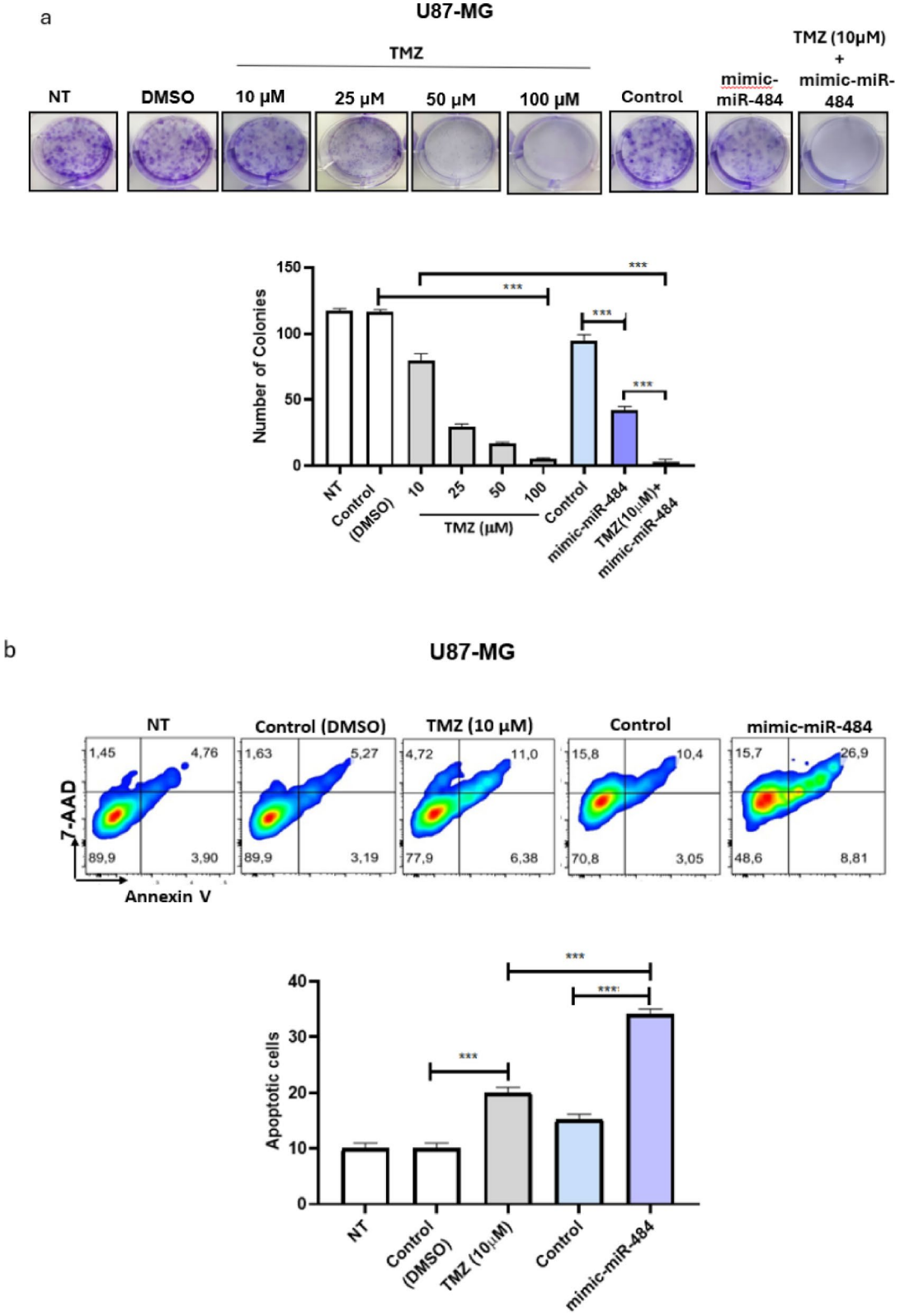

Fig. 5 (See legend on next page.)

(See figure on previous page.)

Fig. 5 Expression of miR-484 increases sensitivity of cells to TMZ. (**a**) U87-MG cells were treated with increasing concentration of TMZ, transfected with mimic-miR-484, combined with TMZ (10 μM) and mimic-miR-484, and evaluated for colony formation. (**b**) Effects of increasing concentration of TMZ and transfection with mimic-miR-484 on apoptosis was examined by annexin V/PI staining. Positively stained cells were quantified with BD FACSARIAIII. A representative flow cytometry plots are shown. (**c**) Expression of miR-484 leads to a reduction in the number of cells in the G1 phase of the cell cycle and an increase in the number of cells in the G2/M phase (**d**) miR-484 expression combined with TMZ leads to increased FOXM1, Integrin β1 and PARP inhibition. U87-MG cells were treated with TMZ (40 μM), transfected with mimic-miR-484 and combined with TMZ (40 μM) and mimic-miR-484. Protein extracts were isolated 72 h after transfection. β-actin was used as a loading control. Band intensities were evaluated by densitometric analysis. The group control represents cells transfected with the control-miRNA (*$P < 0.05$, **$P < 0.01$, and ***$P < 0.001$)

more colony formation against U-87 MG cells than each treatment alone (Fig 5 a).

To determine the effect of miR-484 on induction apoptosis and cell cycle, we performed a flow cytometry analysis following Annexin V/PI staining of U87-MG (Fig 5b-c). miR-484 mimic and TMZ significantly increased the number of apoptotic cells (Fig 5b). The cell cycle analysis revealed a reduced number of cells in G1 phase, resulting in an increase in the number of cells in the G2/M phase after mimic-miR-484 transfection (Fig 5c). These results demonstrated that expression of miR-484 in cells increased apoptosis as seen after TMZ treatment and had an impact on cell cycle.

Finally, we investigated the mechanism by which mimic-miR-484 a sensitizes to TMZ and investigated expression of FOXM1 and its downstream targets proteins in GBM cells. We found that FOXM1 and the expression of its downstream target proteins, including Integrin-β1, p-Src, cyclin-D, and PARP, were dramatically increased in GBM cells after 72 h of treatment with TMZ alone. However, as shown in Fig 5d, combination mimic-miR-484 with TMZ led to marked inhibition of FOXM, Integrin- β1 phosphorylation of Src and DNA-repair enzyme PARP in U87-MG cells compared to each treatment alone.

Overall, our results indicate that the combined therapy of TMZ and mimic-miR-484 effectively downregulates the FOXM1 axis in GBM cells (Fig 5d) and enhances their sensitivity to TMZ. This suggests that combining miR-484 mimic with TMZ could lead to increased therapeutic efficacy of TMZ by potentially resensitizing GBM cells through FOXM1 downregulation.

Pathways associated with miR-484

To determine the role of miR-484 in GBM cells, we performed Gene Ontology (GO) enrichment analysis and Kyoto Encyclopedia of Genes and Genomes (KEGG) pathway analysis using DIANA Tools mir-Path.v3 (Tarbase), a web-based computational tool [30, 37]. GO analysis revealed 67 targets that were primarily involved in cell death, cell motility, cell cycle (cut off, $p < 0.05$, Table S2). Analysis of the KEGG pathway revealed enrichment in 8 pathways including glioma, adherent's junction, focal adhesion, cell cycle (cut off, $p < 0.05$, Table S3). The detailed results of GO and KEGG analyses for miR-484 were presented in Table S 2–3. The KEGG pathway and the GO enrichment analysis indicated that miR-484 were associated with cancer initiation and progression.

FOXM1 inhibits expression of tumor suppressor miR-484 in GBM cells

Our previous study demonstrated that FOXM1 induces the expression of oncogenic miRNAs (miR200b) and inhibits the expression of the tumor suppressor miRNA-186 in breast cancer cells [30]. Therefore, to examine whether link between the oncogenic transcription factor FOXM1 and miR-484 expression, we first utilized the TransmiR v2.0 database [38]. TransmiR is a database of transcription factor (TF)-microRNA (miRNA) regulations that allows users to find regulatory relationships between TFs and miRNAs [30, 38]. In the current study, TransmiR v2.0 database analysis demonstrated a potential transcriptional regulation between FOXM1 and miR-484 (Fig 6a, b). illustrates the regulatory relationship between the transcription factor FOXM1 and hsa-mir-484, suggesting that FOXM1 may regulate the expression of hsa-mir-484 by binding to specific sites on chromosome 16 near the hsa-mir-484 gene's transcription start site.

To verify these in silico findings, we evaluated the miR-484 expression profile in IDH-wild type U-87 cells transfected with FOXM1 or control siRNAs using qRT-PCR. Our results showed that miR-484 was significantly upregulated in cells transfected with FOXM1 siRNAs compared to cells transfected with control siRNA (Fig 6c). These results confirmed the transcriptional regulation between FOXM1 and miR-484 identified by the TransmiR v2.0 database, establishing FOXM1 as a transcriptional repressor of miR-484 in GBM cells.

Then, we performed target analysis using the Mirwalk tool (http://mirwalk.umm.uni-heidelberg.de/human/interaction/21414864/) In silico data showed a stable and specific binding between miR-484 and FOXM1, supported by a highly negative binding energy (negative binding energy = -25.4\ kcal/mol) and a a strong binding score (binding score = 0.846). Specifically, the analysis indicated that miR-484 binds to the 5' Untranslated Region (5' UTR) of the FOXM1 mRNA. This highly binding energy indicates a strong potential for miR-484 to target and regulate FOXM1 expression (Fig 6d).

Taken together, our results indicate that FOXM1, as an oncogenic transcription factor, has a significant

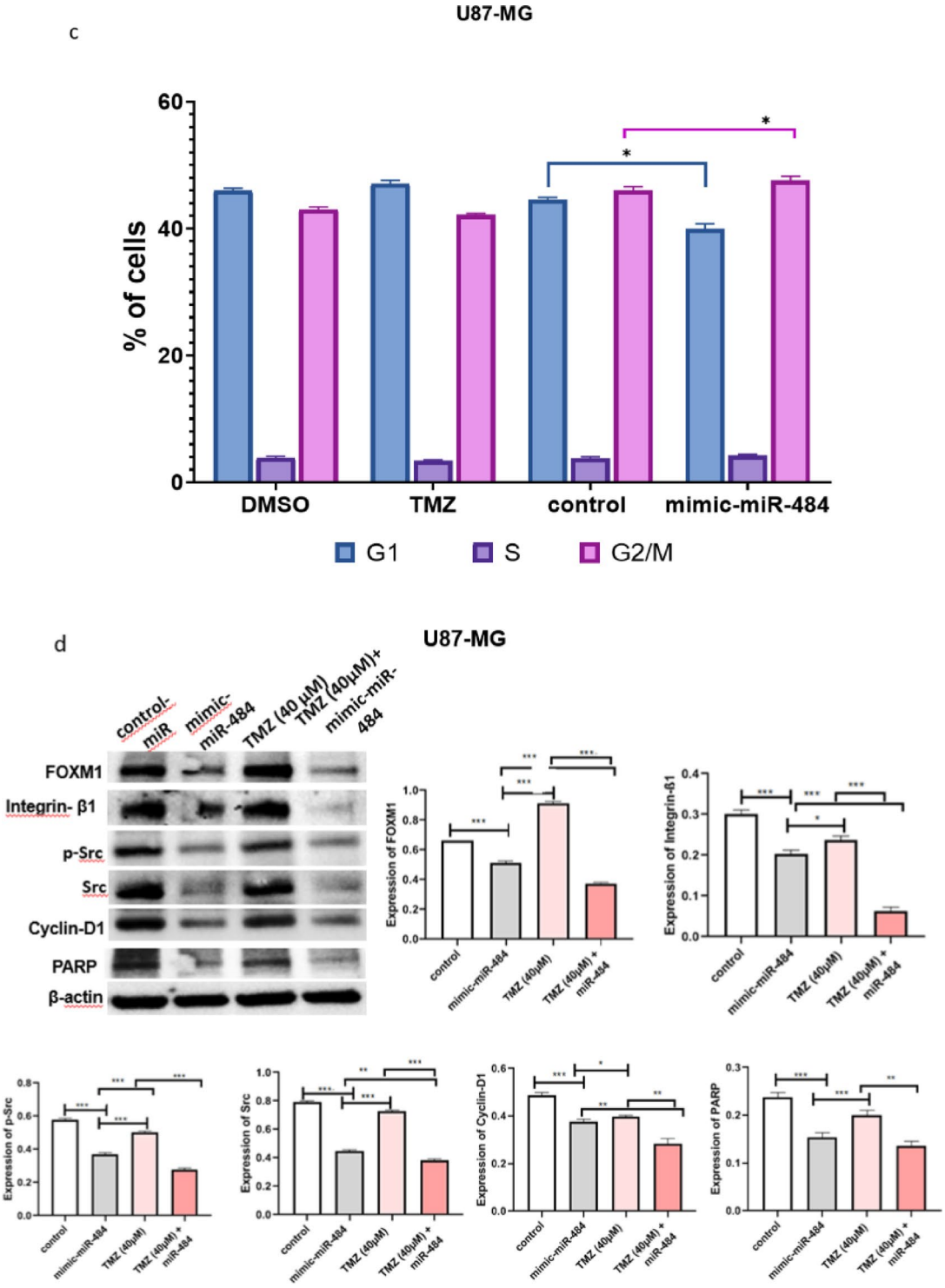

Fig. 5 (continued)

repressive effect on miR-484 expression in GBM cells. This suggests that increased FOXM1 expression leads to the inhibition of miR-484 expression, and the resulting downregulation of miR-484 is associated with poor prognosis in GBM.

Transcriptomic profiling

In our study, we performed RNA sequencing (RNA-seq) analysis to determine the gene expression profile in U87-MG and IDH1-mutant-U87 cells after mimic-miR-484 transfection.

a

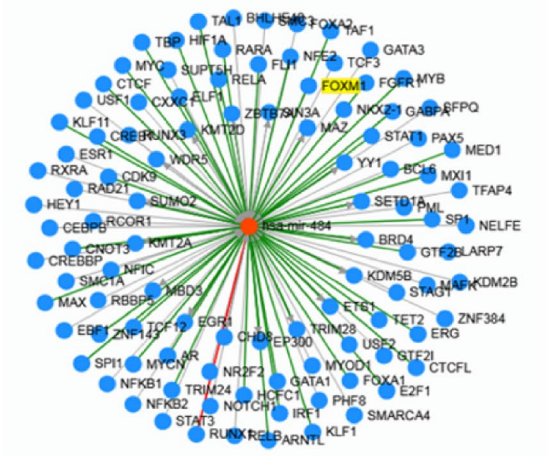

c

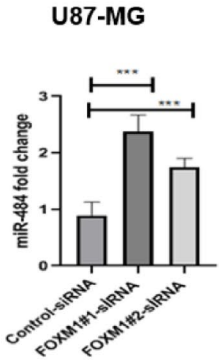

b

TF name	miRNA name	TSS Binding site (Score)	Action type	Tissue
FOXM1	hsa-mir-484	chr16: 15638594 chr16: 15643489-15643783 (score=572)	Regulation	Blood
FOXM1	hsa-mir-484	chr16: 15638594 chr16: 15643527-15643780 (score=521)	Regulation	Blood
FOXM1	hsa-mir-484	chr16: 15638594 chr16: 15643528-15643730 (score=485)	Regulation	Uterus
FOXM1	hsa-mir-484	chr16: 15638594 chr16: 15643557-15643721 (score=564)	Regulation	Breast

d

Details

MiRNA	hsa-miR-484
RefseqID	NM_202002
GeneSymbol	FOXM1
Binding site	230,254
Score	0.846
Seed	1
Au	0.397
Energy	-25.4
Binding len	24
Me	-3.938
Phylopstem	0.06017936842105263
Phylopflank	0.026603675000000007
Longest consecutive pairings	7
Position of longest consecutive pairings	1
Pairings in 3prime end	5
Position	5UTR

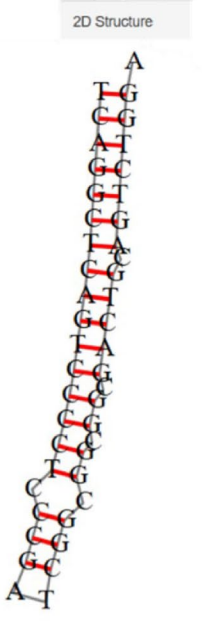

Fig. 6 (See legend on next page.)

(See figure on previous page.)

Fig. 6 Relation between FOXM1 and miR-484. (**a**-**c**) Transcriptional network between the miR-484 and the oncogenic transcription factor FOXM1 was identified using TransmiR v2.0 (http://www.cuilab.cn/transmir) (miR-484 was used as an input). TF name:Transcription Factor name, which is FOXM1;miRNA name: This column specifies the name of the microRNA that FOXM1 is predicted to regulate, which is hsa-mir-484;TSS (Transcription Start Site):This column shows the genomic coordinates of the transcription start site for the hsa-mir-484 gene.TSS is located on chromosome 16 at position 15,638,594; Binding site: This column provides the genomic coordinates of the predicted binding site of FOXM1 on chromosome 16. The coordinates indicate the start and end positions of the binding region; Score: This column represents a score associated with the predicted binding site..The scores range is from 485 to 572; Action type: This column describes the predicted type of action of FOXM1 on hsa-mir-484. FOXM1 is predicted to regulate the expression of hsa-mir-484; Tissue: This column specifies the human tissue in which the predicted binding interaction was observed or is relevant. (d) miRWalk tool analysis showed a stable and specific binding between mir-484 and the 5'UTR region of the FOXM1 mRNA (binding energy = -25.4 kcal/mol) (http://mirwalk.umm.uniheidelberg.de/human/interaction/21414864/)

Our analysis showed that FOXM1 gene expression was downregulated in both U87-MG (Fig 7a) and IDH1-mutant-U87 (Fig 7c) cells after transfection with mimic-miR-484, when compared to cells transfected with control-miR (Fig 7b-d). We also found that FOXM1 gene expression levels were similar between non-transfected (NT) cells and those transfected with control-miR (Fig 7b-d). These results corroborate our Western blot analysis and clearly demonstrate that mimic-miR-484 plays a role in regulating FOXM1 expression.

Figure 8a presents the top 10 most significantly altered GO in U87-MG cells (Fig 8a). Additionally, KEGG pathway analysis reveals the pathways that are upregulated (Fig 8b) and downregulated (Fig 8c). Based on the results of the performed analysis, no statistically significant ($P < 0.05$) ontology was detected in IDH1-mutant-U87cells. Pathway analysis could not be performed for this comparison in IDH1-mutant-U87 cells due to the insufficient number of genes exhibiting significant differential expression (FDR < 0.05).

As a result, Fig 8a represents a GO enrichment analysis performed on the RNA-seq data from the U87-MG cells after mimic-miR-484 transfection, as suggested by the context of the previous statements (Fig. 8a for U87-MG cells). Supplementary Table 2, on the other hand, states it is a "GO enrichment analysis of predicted targets of miR-484, suggesting it might be an *in-silico* prediction of miR-484 targets rather than an analysis of experimental RNA-seq data. Therefore, while both analyses relate to GO analysis and miR-484, they are derived from different types of analyses (experimental RNA-seq data vs. predicted miRNA targets) and thus present different sets of enriched GO terms. Similarly, Fig 8b-c depict the KEGG pathways that are empirically enriched (upregulated and downregulated) based on the differential gene expression observed in the RNA-seq experiment on U87-MG cells after mimic-miR-484 transfection. In contrast, Supplementary Table 3 provides KEGG pathways that are statistically enriched among genes predicted to be targets of miR-484 based on a computational analysis (DIANA miRPath.v3 and Tarbase). Therefore, these sets of results complement each other by showing both the observed biological consequences of mimic-miR-484 transfection and the predicted direct target effects of miR-484 at the pathway level.

Discussion

Several microRNAs have been identified as key players in glioma pathogenesis, and some miRNAs can serve as biomarkers in GBM [39]. For example, oncogenic microRNAs such as miR-21[40], and miR-24 [41] are frequently upregulated in GBM while numerous tumor suppressors microRNAs such as miR-429 [42], miR-181 [40] are downregulated. Presented in our study, we found that miR-484 was low expressed in IDH-wild type compared to IDH-mutant patient's tissue samples. Furthermore, we demonstrated that increased expression of miR-484 by mimic-miR-484 led to an inhibition of colony formation, migration, and invasion, and an induction of apoptosis in IDH-wild type and IDH-mutant cells. Moreover, results of the current study demonstrated for the first time that expression of miR-484 suppressed oncogenic FOXM/Integrin-β1/Src/Fak and cyclin-D1 signaling axis and PARP expression in GBM cells. In addition, expression of miR-484 increased TMZ- induced cell death in GBM U-87 cells. Our findings indicate that miR-484 may function as a tumor suppressor in GBM.

Similarly, miR-484 is overexpressed in hepatocellular carcinoma, where its high expression targets the tumor suppressor gene TUSC5, thereby promoting cell proliferation, metastasis, and progression of the disease [43]. Similarly, high miR-484 expression acts as a candidate oncogene in the development, progression, and recurrence of prostate cancer by targeting potential tumor suppressors like PSMG1 [44]. In non-small-cell lung cancer (NSCLC), high miR-484 expression is associated with diagnosis, prognosis, and lower patient survival rates. miR-484 has also been found to enhance migration and proliferation while inhibiting apoptosis in NSCLC cells by down-regulating Caspase-3, Apaf-1, and PARP cleavage [19, 45]. Furthermore, miR-484 is relevant in breast cancer prognosis; Shi et al. [20] reported that higher hsa-miR-484 expression correlated with worse prognosis in patients with invasive breast cancer. Another study found significantly higher serum levels of miR-484 in early breast cancer patients compared to healthy volunteers [46]. In our previous study, we observed that miR-484

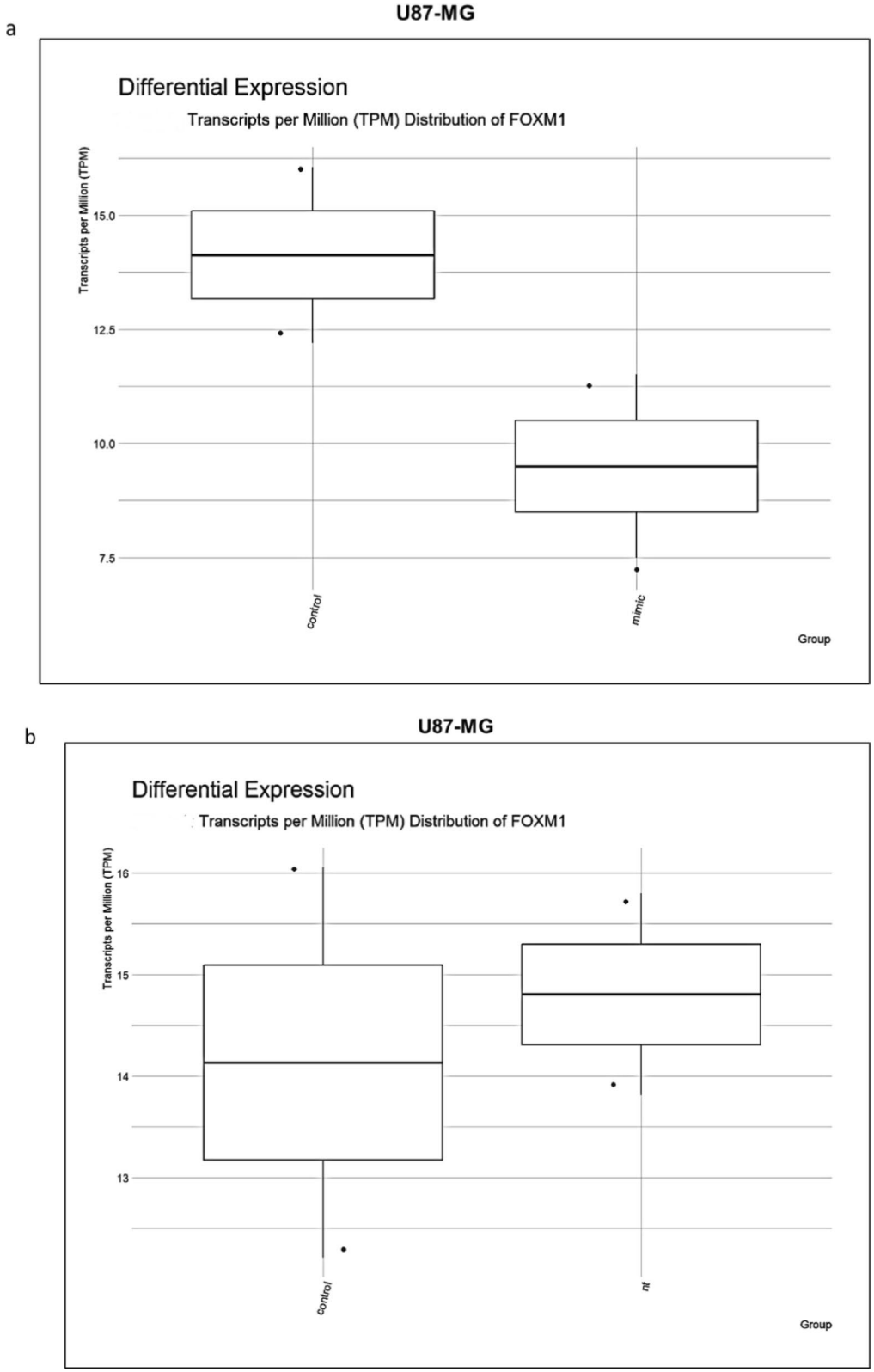

Fig. 7 Differential Expression of FOXM1 in U87-MG and IDH1-mutant U87 cells. (**a**) FOXM1 expression levels in U87-MG cells transfected with Control-miRNA versus cells transfected with mir-484 mimic. (**b**) FOXM1 expression levels in U87-MG cells transfected with Control-miRNA compared to Non-Transfected (NT) control cells.(**c**) FOXM1 expression levels in IDH1-mutant U87-MG cells transfected with Control-miRNA versus cells transfected with mir-484 mimic. (**d**) FOXM1 expression levels in IDH1-mutant U87-MG cells transfected with Control-miRNA compared to Non-Transfected (NT) control cells

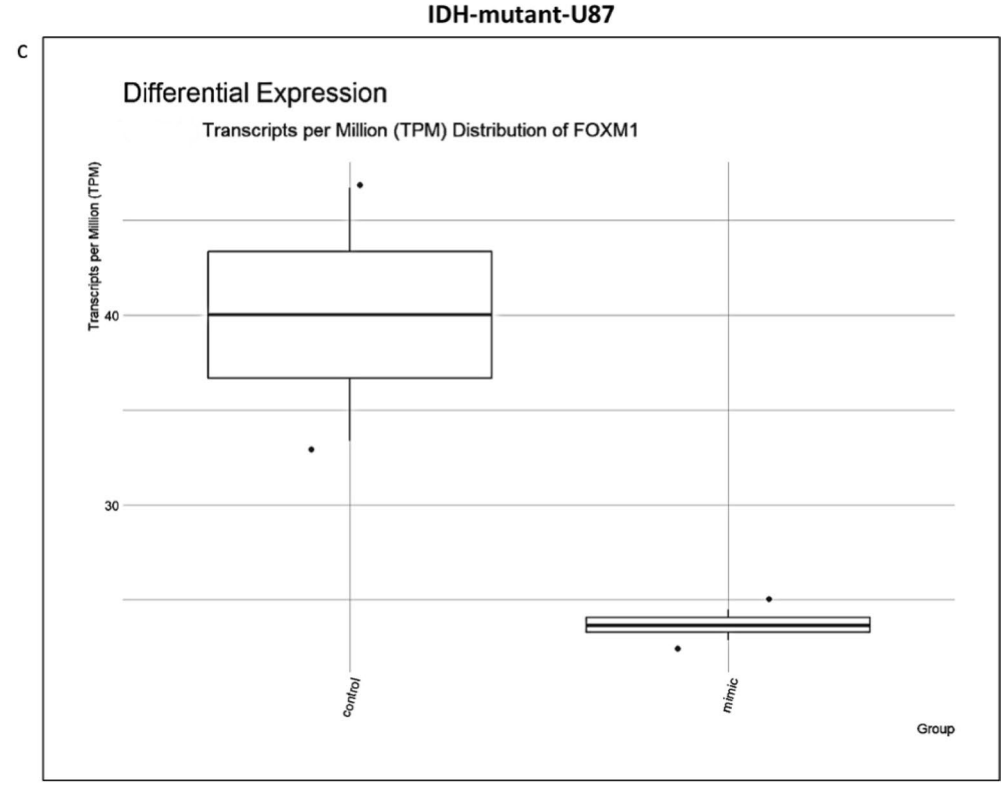

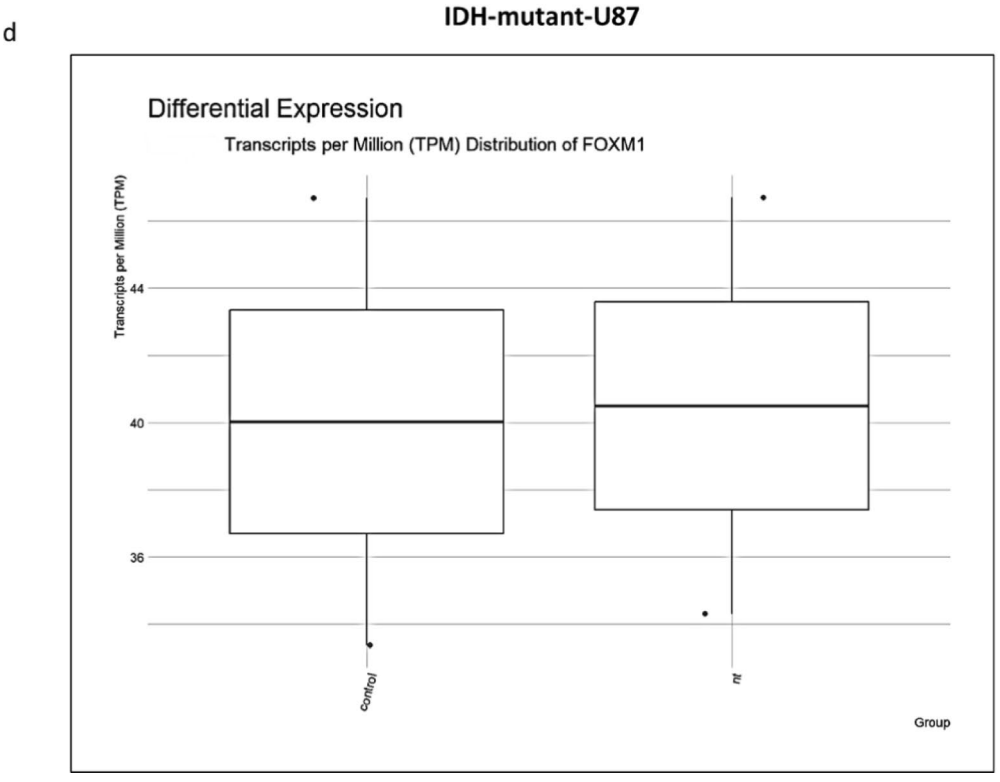

Fig. 7 (continued)

expression was higher in breast tumor tissue samples compared to healthy tissue, and its expression was also elevated in malignant tumors versus benign ones [47]. Volinia et al. [48] also identified a strong association

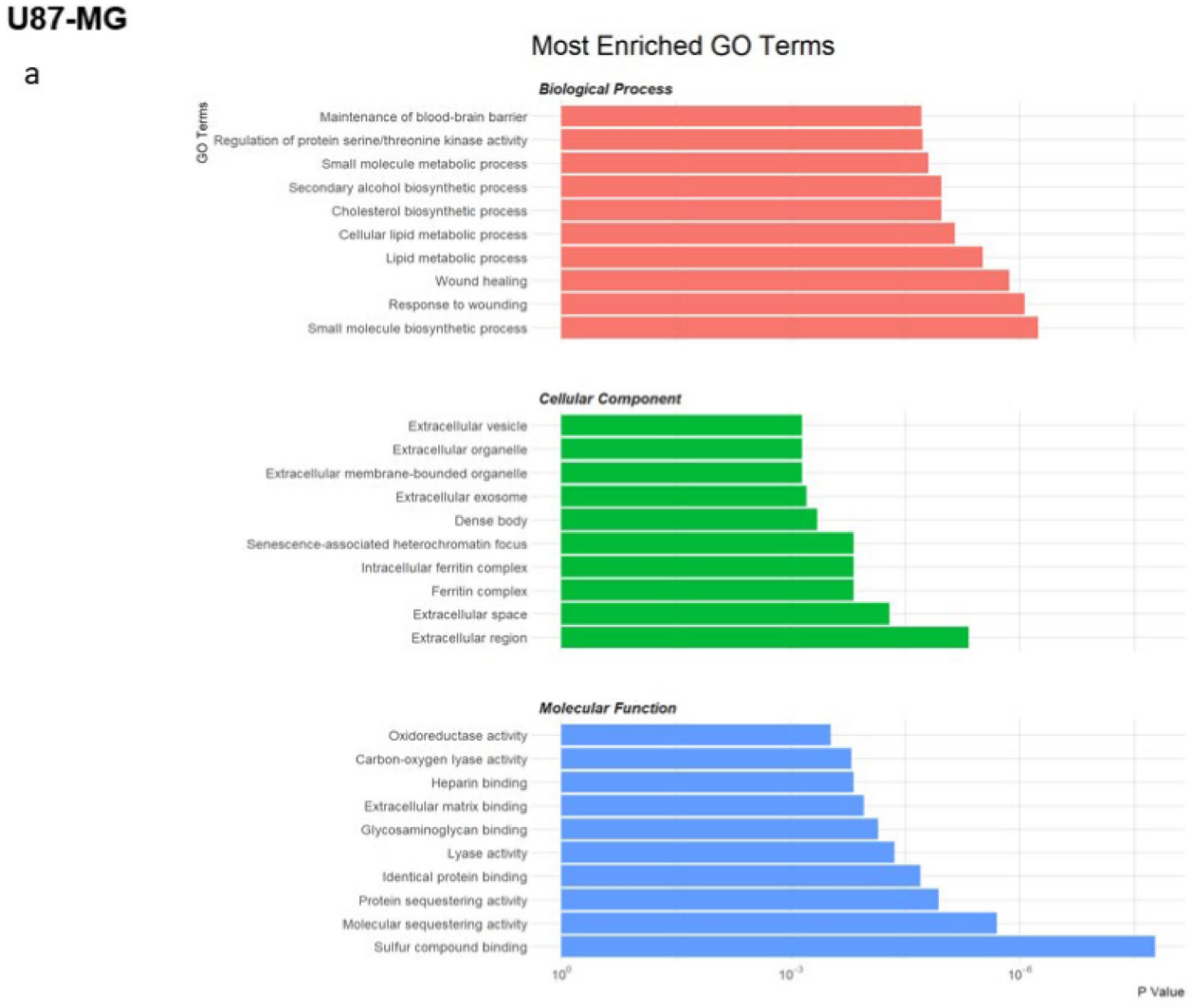

Fig. 8 Significantly variable Gene Ontology (GO) terms and pathways in U87-MG cells. (**a**) Displays the top 10 Gene Ontology (GO) terms exhibiting significant changes, ordered by their statistical significance. The X-axis represents the negative logarithm of the P-value, where a higher value indicates stronger statistical significance for the associated GO term. For this gene ontology analysis, only genes showing a significant difference (FDR < 0.05) between the groups were considered. (**b**) Presents a dot plot visualizing the most significantly upregulated pathways. (**c**) Shows a dot plot illustrating the most significantly downregulated pathways

between miR-484 and the prognosis of patients with primary invasive ductal carcinoma.

Conversely, in other cancers, miR-484 acts as a tumor suppressor. Downregulation of miR-484 is linked to poor prognosis and tumor progression in gastric cancer. Upregulation of miR-484 expression reduced tumorigenicity, suppressed growth and metastasis, and induced apoptosis in gastric cancer cells by inhibiting the CCL-18/PI3K/AKT pathway [14, 15]. Similarly, miR-484 expression was significantly downregulated in colorectal cancer patient tissues compared to their normal colon tissues [49]. Long Non-coding RNAs (lncRNAs) are also implicated in the development of colorectal cancer and renal cell carcinoma by regulating miR-484 expression. For example, it has been shown that downregulation of miR-484 expression, potentially caused by the overexpression of oncogenic lncRNAs like PGM5-AS1 [50]. Additionally, high expression of oncogenic lnc PCED1B-AS1 combined with low miR-484 expression is commonly associated with high tumor stage and shortened overall survival in renal cell carcinoma patients [52]. To our knowledge, the role of mir484 in GBM is unknown. However, Yi et al. [22] investigated effect of miR-484 on glioma stem cells, and found that inhibition of miR-484 decreased tumor sphere size and number of cells positively staining CD 44 and CD133 glioma cancer stem cells (CSCs), suggesting that miR-484 acts as a oncomiR in glioma stem cells. Moreover, miR-484 was shown to directly target MAP2, resulting in activation of ERK1/2 signaling and promote the tumor-initiating capability of stemness

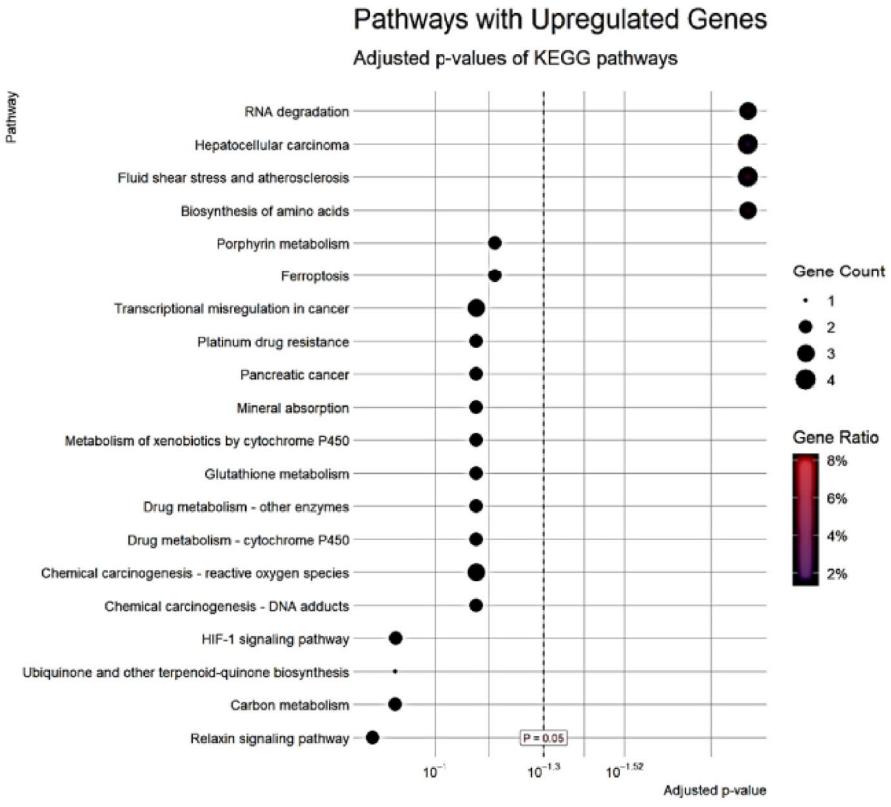

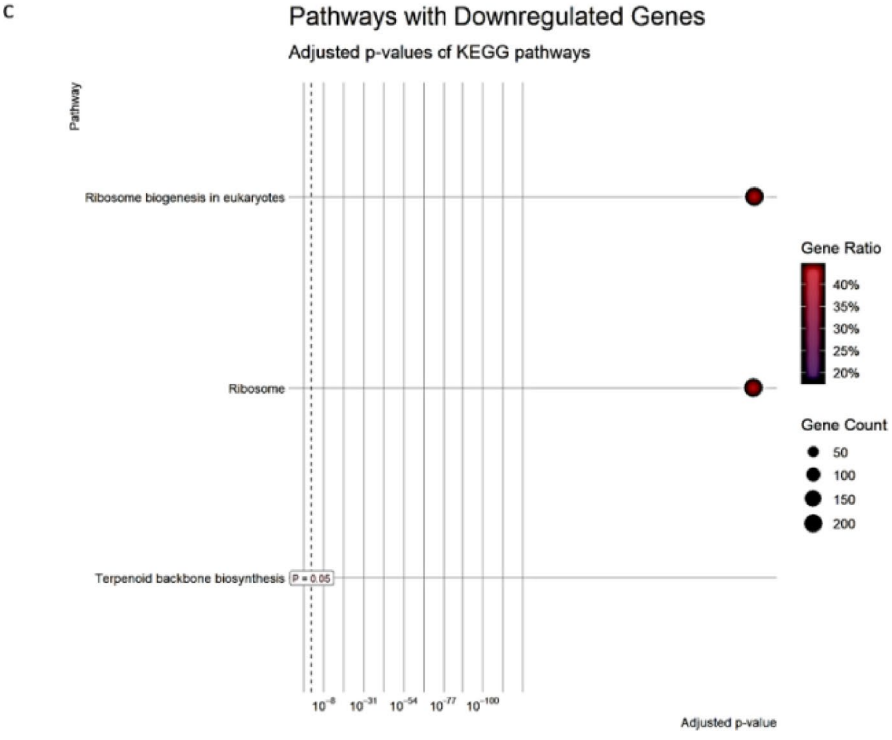

Fig. 8 (continued)

in glioma, and the high expression of miR-484 could promote the initiation of glioma [22]. Another study showed that miR-484 was highly expressed in human glioma cell lines compared to normal astrocytes, with particularly

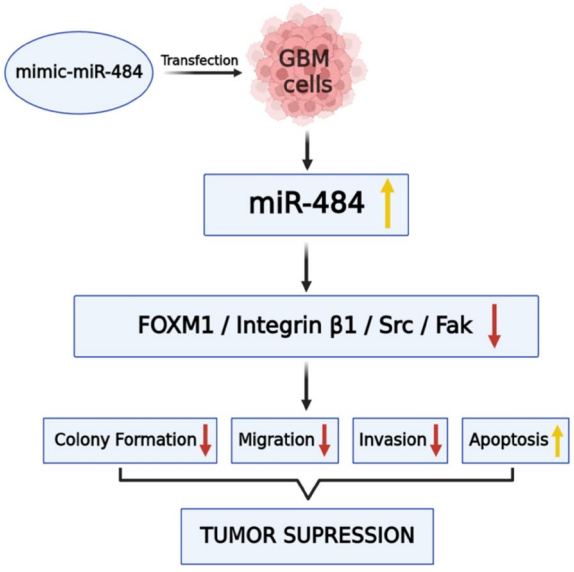

Fig. 9 Blocking of FOXM1 signaling axis with expression of miR-484, contributing to suppresses colony formation, migration and invasion and to induces apoptosis in GBM cells

high expression in LN-229 glioma cells relative to other glioma cell lines (T98G, A172, U-87MG, and U-251MG). This study also demonstrated that miR-484 expression enhanced migration, invasion, and angiogenesis by inhibiting Cyclin Dependent Kinase Inhibitor 2A (CDKN2A) expression in LN-229 cells [23].

Contrary to these findings, we report for the first time that miR-484 expression significantly inhibited cell proliferation, migration, and invasion, and increased apoptosis. Conversely, inhibiting miR-484 did not lead to any change in these phenotypic features in IDH wild-type U87-MG cells and IDH1-mutant U87 cells. Non-transfected (NT) cells, control-miRNA transfected cells, and transfected cells with inhibitor-miR-484 displayed similar miR-484 expression profiles (Fig 3a-b). Therefore, we hypothesize that inhibitor-miR-484 did not affect proliferation, colony formation, migration, or invasion in these cells, likely due to the already low endogenous expression of miR-484. Furthermore, we demonstrated that expression of miR-484 significantly decreased expression of FOXM1 and its downstream mediators including Integrin-β1/Src/Fak and cyclin-D1 and PARP in GBM cells, suggesting that miR-484 exerts anti-cancer effects by targeting the FOXM1/Integrin-β1/Src/Fak signaling pathway. (Graphical Abstract, Fig 9). In conclusion, our findings demonstrate that miR-484 expression exerts an inhibitory effect on GBM progression, supporting its role as a potential tumor suppressor in GBM cells. Similarly, clear cell renal cell carcinoma has shown that miR-484 overexpression suppresses cell proliferation, migration, invasion, and epithelial-mesenchymal transition (EMT), and markedly inhibits the expression of ZEB1 and SMAD2, which are key transcription factors of EMT [51].

Our previous study and others have shown that FOXM1 is highly expressed in GBM U87MG cells and plays a crucial role in inducing cell cycle progression, proliferation, and invasion. [24–26]. Another our study demonstrated that FOXM1 directly or indirectly activates the expression of miRNAs at the transcriptional level, even increased FOXM1 expression leads to induction of oncomiR186 and inhibiting tumor-suppressor miR-200b-5p [30]. Therefore, to better understand the role of miR-484 in GBM cells, we applied bioinformatics analyses to predict relationship between miR-484 and FOXM1 using TransmiR v2.0 database, found a link between miR-484 and FOXM1 expressions. Furthermore, we confirmed that FOXM1 acts as a transcriptional repressor of miR-484 expression in GBM cells, suggesting that high FOXM1 levels contribute to the downregulation of the tumor suppressor miR-484 (Fig 4a-b). miR-484 targets the FOXM1 mRNA via a non-canonical binding mechanism at the 5' UTR (Fig 6d). Also, cBioPortal analysis indicated that while miR-484 exhibits amplification across various cancers (Fig 1g), its downregulation in aggressive IDH-wild type GBM is primarily driven by the transcriptional repression imposed by FOXM1, linking the molecular axis to poor prognosis. We found a strong clinical correlation, showing that miR-484 expression levels were markedly lower in IDH-wild type patient tissues compared to those with the IDH-mutant genotype (Fig 1a). ROC curve analysis demonstrated that miR-484 expression has a robust discriminatory power to distinguish between IDH-mutant and IDH-wild type patients (Fig 2a). Collectively, these findings highlight the FOXM1/miR-484 regulatory axis as a significant pathogenic pathway in gliomas, suggesting that restoring miR-484 levels or inhibiting FOXM1 activity could be a novel therapeutic strategy for IDH-wild type GBM.

Our findings suggest that high FOXM1 expression, as a transcription factor, may significantly affect the regulation of miR-484 expression in GBM. FOXM1, a known oncogenic protein in GBM, may be involved in tumorigenesis by inhibiting miR-484. All of these results suggest that enhanced FOXM1 expression may inhibit the expression of miR-484 at the transcriptional level in GBM. However, further research, including experimental validation using techniques such as luciferase reporter and ChIP assays, is necessary to definitively confirm a direct or indirect regulatory relationship between hsa-mir-484 and FOXM1, and to fully elucidate the specific biological roles and impacts of this interaction in GBM.

Previous our study demonstrated that FOXM1 transcription factor regulates Integrin-β1 expression and its downstream FAK signaling pathway which promotes cell invasion [35], as well as Cyclin D1 which plays a key role

in entry into G1 phase. The expression of integrin β1, the activation and phosphorylation of FAK and Src have all been shown to play a role in the progression of GBM [52–54]. Cyclin D1 is a major regulator of cell cycle progression in GBM [55]. Here in our study, we demonstrated that expression of miR-484 lead to decrease expression of Cyclin-D1 protein, which is a downstream target of FOXM1. Moreover, in our analysis of KEGG pathway and GO analyses shown that mir-484 are involved cell cycle, cell motility, focal adhesion and glioma pathways supporting our findings.

Interestingly, miR-484 exhibits a contrasting role in NSCLC compared to our findings in GBM. In NSCLC, high miR-484 expression has been shown to promote cell proliferation and migration, partly through the inhibition of PARP [19] and by blocking apoptosis via Apaf-1 downregulation, ultimately leading to PARP activation and disease progression [19].

Conversely, our results in GBM demonstrate that increased miR-484 expression, achieved through FOXM1 inhibition, significantly inhibits PARP expression and promotes apoptosis. Given the established role of PARP in DNA repair and its association with GBM drug resistance and poor prognosis [56], our findings suggest that our findings suggest that miR-484 may suppressor oncogenic activity of PARP in GBM. While PARP inhibitors are being explored to overcome drug resistance in GBM [56, 57], our data indicate that miR-484 upregulation might contribute to this sensitization by directly targeting PARP through FOXM1 modulation, highlighting a potential therapeutic strategy unique to GBM.

Currently, the DNA-alkylating agent temozolomide (TMZ) is the most widely used chemotherapeutic drug for the treatment of GBM patients. However, the development of acquired resistance to TMZ represents a major challenge in GBM therapy [58]. miR-484 was linked with resistance to chemotherapeutic agents in cancer. Prior et al. [59] showed that the expression of miR-484 has been closely related to metastatic renal cell carcinoma treated with sunitinib, and miR-484 was overexpressed in sunitinib-resistant patients. Our results similarly demonstrated that miR-484 expression increased TMZ-induced cell death, suggesting that miR-484 modulates chemosensitivity to TMZ by targeting FOXM1 in GBM cells. These findings indicate that combining mimic-miR-484 with TMZ can overcome TMZ resistance, a major clinical challenge in GBM treatment, and lead to greater therapeutic benefit, potentially improving patient responses to this standard chemotherapy.

The ability of GBM cells to repair DNA damage is a major contributor to their resistance to TMZ [60]. Our study demonstrated that TMZ treatment increased FOXM1 expression in U87 cells, an observation consistent with other reports in GBM [61]. Therefore, the TMZ-induced upregulation of FOXM1 suggests a potential mechanism by which GBM cells attempt to counteract the cytotoxic effects of TMZ, thereby contributing to drug resistance.

Mutant IDH enzyme converts αKG (α-ketoglutarate (α-KG, 2-oxoglutarate, 2-OG) to 2-HG, leading to an increased concentration of 2-hydroxyglutarate (2-HG) in cells [62–64]. The metabolic consequences derived from IDH mutations alter cellular epigenetics, metabolism, DNA hypermethylation, DNA repair pathways, and the expression of tumor suppressors and oncogenes. Specifically, the epigenetic changes induced by the mutant IDH enzyme's product lead to distinct differences between wild-type IDH1 and IDH1-mutant gliomas. IDH1-mutant GBM cells exhibit metabolic and epigenetic reprogramming that differs from wild-type IDH1 cells, depending on the specific IDH gene mutation [63, 64]. Therefore, we think that the observed partial differences in protein expression between U87-MG and IDH1-mutant-U87 GBM cells transfected with miR-484 (Fig 3c-u) may be associated with the metabolic consequences of IDH mutations.

Given that miR-484 can act as both an oncogene and a tumor suppressor, further research is needed to elucidate its specific regulatory mechanisms in cancer cells. Similarly, our observation of partially different cell migration and invasion responses to mimic miR-484 transfection in IDH-wild type and IDH-mutant cells suggests that these differences may be associated with the metabolic and epigenetic consequences of IDH mutations. These mutations, depending on their presence or absence, can influence cell motility and invasiveness. One of the limitations of our study is that we used only a single cell line for the mutated cells. Use of other IDH1 mutated cell lines may further confirm our results and solidify the conclusion.

In summary, all of our results indicated that miR-484 may functions as tumor suppressor miRNA in GBM cells by inhibiting clinically significant pathways including FOXM1/integrin-β1/FAK/Src and Cyclin-D and PARP (Fig 9). Use of miR484 mimic may provide a new avenue to overcome chemoresistance in GBM. Furthermores, use of mimic miR-484 in GBM cells leads to reduced cell proliferation, migration, invasion, and induction of apoptotic cell death, indicating that miR-484-based therapy may be a potential treatment strategy of GBM patients., our study established a critical regulatory link between the oncogenic transcription factor FOXM1 and the tumor suppressor miR-484 in Glioblastoma (GBM) cells, demonstrating the clinical significance of miR-484 expression in gliomas. However, we suggest that in vivo studies using GBM tumor models are needed to explore the role of miR-484, and determine whether a therapeutic approach targeting miR-484 is effective for controlling GBM tumor growth and progression.

Supplementary Information

The online version contains supplementary material available at https://doi.org/10.1186/s12935-026-04238-x.

Supplementary Material 1

Supplementary Material 2

Supplementary Material 3

Supplementary Material 4

Supplementary Material 5

Supplementary Material 6

Supplementary Material 7

Supplementary Material 8

Supplementary Material 9

Supplementary Material 10

Supplementary Material 11

Supplementary Material 12

Supplementary Material 13

Supplementary Material 14

Acknowledgements
Thanks to all those who helped in data preparation and paper writing.

Author contributions
All authors analyzed the results and approved the final version of the manuscript. **Zuhal Hamurcu**: conceptualized, coordinated, administered the study, performed experiments, and wrote the paper. **Bulent Ozpolat**: conceived, conceptualized, supervised the study and revised and edited the manuscript. **Nursultan Nurdınov, Ahsen Guler, Serhat Albayrak, Venhar Cınar, Mehmet Memiş, Serife Erdem, Gizem Kusunluoglu**: helped performing the experiments. **Halil Ulutabanca**: coordinated obtaining and use of patient samples. **Elif Funda Sener and Serpil Taheri**: analyzed and interpreted miR-484 expression data. **Omer Aydın:** helped writing the paper.

Funding
This study was supported by Erciyes University Research Fund (grant numbers: TDK-2019–9172, TYL-2022–11870 and THD-205–14690) and The Scientific and Technological Research Council –TÜBİTAK- research grant (grant number: 119S935).

Data availability
No datasets were generated or analysed during the current study.

Declarations

Ethics approval
This study was approved by Clinical Research Ethics Committee of Erciyes University (ethical approval Protocol No. 2019/247) and implemented in accordance with the Helsinki Declaration of Principles.

Informed consent
GBM cancer samples were obtained from Erciyes University Medical Faculty Hospital, Neurology Department. All patients provided their signatures on the written informed consent document (decision no: 2019/247).

Competing interests
The authors declare no competing interests.

Author details
[1]Faculty of Medicine, Department and of Medical Biology, Erciyes University, Kayseri 38039, Turkey
[2]Betül-Ziya Eren Genome and Stem Cell Center, Erciyes University, Kayseri 38039, Turkey
[3]Faculty of Medicine and Dentistry, Ahmet Yassawi International Kazakh-Turkısh University, Turkestan Z05K7B0, Kazakhstan
[4]Gevher Nesibe Genome and Stem Cell Institute, Erciyes University, Kayseri 38039, Turkey
[5]Nanothera Lab, Drug Application and Research Center (ERFARMA), Erciyes University, Kayseri 38039, Turkey
[6]Faculty of Medicine, Department of Neurosurgery, Erciyes University, Kayseri, Turkey
[7]Institute of Health Sciences, Erciyes University, Kayseri, Turkey
[8]Department of Immunology, School of Medicine, Kırsehir Ahi Evran University, Kırsehir, Turkey
[9]Department of Biomedical Engineering, Erciyes University, Kayseri 38039, Turkey
[10]Stephenson School of Biomedical Engineering, The University of Oklahoma, Norman, OK 73019, USA

Received: 21 June 2025 / Accepted: 16 February 2026
Published online: 01 April 2026

References

1. Weller M, Wen PY, Chang SM, Dirven L, Lim M, Monje M, et al. Glioma. Nat Rev Dis Primers. 2024. https://doi.org/10.1038/s41572-024-00516-y.
2. Louis DN, Perry A, Reifenberger G, et al. The 2016 World Health Organization classification of tumors of the central nervous system: a summary. Acta Neuropathol. 2016. https://doi.org/10.1007/s00401-016-1545-1.
3. Motomura K, Kibe Y, Ohka F, Aoki K, Yamaguchi J, Saito R. Clinical characteristics and radiological features of glioblastoma, IDH-wildtype, grade 4 with histologically lower-grade gliomas. Brain Tumor Pathol. 2023. https://doi.org/10.1007/s100-023-00458-5.
4. Ruiz MF, Gennaro MV, Bastone LC, Godoy AR, Torruella M, Perez GR. Molecular biomarkers and integrated pathological diagnosis in the reclassification of gliomas. Mol Clin Oncol. 2021. https://doi.org/10.3892/mco.2021.2312.
5. Gupta M, Anjari M, Brandner S, Fersht N, Wilson E, Thust S, et al. Isocitrate dehydrogenase 1/2 wildtype adult astrocytoma with WHO grade 2/3 histological features: molecular re-classification, prognostic factors, clinical outcomes. Biomedicines. 2024. https://doi.org/10.3390/biomedicines12040901.
6. Ge M, Zhu Y, Wei M, Piao H, He M. Improving the efficacy of anti-EGFR drugs in GBM: Where we are going? Biochim Biophys Acta Rev Cancer. 2023. https://doi.org/10.1016/j.bbcan.2023.188996.
7. Nozhat Z, Heydarzadeh S, Shahriari-Khalaji M, Wang S, Iqbal MZ, Kong X. Advanced biomaterials for human glioblastoma multiforme (GBM) drug delivery. Biomater Sci. 2023. https://doi.org/10.1039/d2bm01996e.
8. Zheng Y, Ma X, Feng S, Zhu H, Chen X, Yu X, et al. Dendritic cell vaccine of gliomas: challenges from bench to bed. Front Immunol. 2023. https://doi.org/10.3389/fimmu.2023.1259562.
9. Behrooz AB, Latifi-Navid H, Nezhadi A, Świat M, Los M, Jamalpoor Z, et al. Molecular mechanisms of microRNAs in glioblastoma pathogenesis. Biochim Biophys Acta Mol Cell Res. 2023;1870:119482. https://doi.org/10.1016/j.bbamcr.2023.119482.
10. Rahmani F, Hashemian P, Tabrizi AT, Ghorbani Z, Ziaeemehr A, Alijannejad S, et al. Regulatory role of miRNAs on Wnt/β-catenin signaling in tumorigenesis of glioblastoma. Indian J Cancer. 2023. https://doi.org/10.4103/ijc.IJC_251_21.
11. Sell MC, Ramlogan-Steel CA, Steel JC, Dhungel BP. Micrornas in cancer metastasis: biological and therapeutic implications. Expert Rev Mol Med. 2023. https://doi.org/10.1017/erm.2023.7.
12. Pagoni M, Cava C, Sideris DC, Avgeris M, Zoumpourlis V, Michalopoulos I, et al. MiRNA-based technologies in cancer therapy. J Pers Med. 2023. https://doi.org/10.3390/jpm13111586.
13. Rosolen D, Nunes-Souza E, Marchi R, Tofolo MV, Antunes VC, Berti FCB, et al. MiRNAs action and impact on mitochondria function, metabolic reprogramming and chemoresistance of cancer cells: a systematic review. Biomedicines. 2023. https://doi.org/10.3390/biomedicines11030693.
14. Liu J, Li SM. MiR-484 suppressed proliferation, migration, invasion and induced apoptosis of gastric cancer via targeting CCL-18. Int J Exp Pathol. 2020. https://doi.org/10.1111/iep.12366.

15. Li Y, Liu Y, Yao J, Li R, Fan X. Downregulation of miR-484 is associated with poor prognosis and tumor progression of gastric cancer. Diagn Pathol. 2020. https://doi.org/10.1186/s13000-020-00946-8.
16. Lin T, Pu X, Zhou S, Huang Z, Chen Q, Zhang Y, et al. Identification of exosomal miR-484 role in reprogramming mitochondrial metabolism in pancreatic cancer through Wnt/MAPK axis control. Pharmacol Res. 2023. https://doi.org/10.1016/j.phrs.2023.106980.
17. Wei Y, Li H, Qu Q. miR-484 suppresses endocrine therapy-resistant cells by inhibiting KLF4-induced cancer stem cells in estrogen receptor-positive cancers. Breast Cancer. 2021. https://doi.org/10.1007/s12282-020-01152-6.
18. Lee D, Tang W, Dorsey TH, Ambs S. miR-484 is associated with disease recurrence and promotes migration in prostate cancer. 2020. Biosci Rep. https://doi.org/10.1042/BSR20191028.
19. Li T, Ding ZL, Zheng YL, Wang W. MiR-484 promotes non-small-cell lung cancer (NSCLC) progression through inhibiting Apaf-1 associated with the suppression of apoptosis. Biomed Pharmacother. 2017. https://doi.org/10.1016/j.biopha.2017.09.10.
20. Yang Y, Lin X, Lu X, Luo G, Zeng T, Tang J, et al. Interferon-microrna signalling drives liver precancerous lesion formation and hepatocarcinogenesis. Gut. 2016. https://doi.org/10.1136/gutjnl-2015-310318.
21. Ye FG, Song CG, Cao ZG, Xia C, Chen DN, Chen L, et al. Cytidine Deaminase Axis modulated by miR-484 differentially regulates cell proliferation and chemoresistance in breast cancer. Cancer Res. 2015. https://doi.org/10.1158/0008-5472.CAN-14-2341.
22. Yi R, Feng J, Yang S, Huang X, Liao Y, Hu Z, et al. miR-484/MAP2/c-Myc-positive regulatory loop in glioma promotes tumor-initiating properties through ERK1/2 signaling. J Mol Histol. 2018. https://doi.org/10.1007/s10735-018-9760-9.
23. Gu Y, Lei H, Ma P, Chen Y. MiR-484 promotes the malignant progression of glioma by inhibiting CDKN2A expression. Folia Neuropathol. 2023. https://doi.org/10.5114/fn.2023.130002.
24. Swati K, Varma SR, Parameswari RP, Panda SP, Agrawal M, Prakash A, et al. Computational exploration of FOXM1 inhibitors for glioblastoma: an integrated virtual screening and molecular dynamics simulation study. J Biomol Struct Dyn. 2024. https://doi.org/10.1080/07391102.2024.2308772.
25. Xu K, Zhang K, Ma J, Yang Q, Yang G, Zong T, et al. CKAP4-mediated activation of FOXM1 via phosphorylation pathways regulates malignant behavior of glioblastoma cells. Transl Oncol. 2023. https://doi.org/10.1016/j.tranon.2023.101628.
26. Zhao P, Li T, Wang Y, Wang Y, Gu Q, Li Z. LncRNA MYCNOS promotes glioblastoma cell proliferation by regulating miR-216b/FOXM1 axis. Metab Brain Dis. 2021. https://doi.org/10.1007/s11011-021-00729-0.
27. Jia YZ, Liu J, Wang GQ, Song ZF. miR-484: a potential biomarker in health and disease. Front Oncol. 2022. https://doi.org/10.3389/fonc.2022.830420.
28. Cınar V, Hamurcu Z, Guler A, Nurdinov N, Ozpolat B. Serotonin 5-HT7 receptor is a biomarker poor prognostic factor and induces proliferation of triple-negative breast cancer cells through FOXM1. Breast Cancer. 2022. https://doi.org/10.1007/s12282-022-01391-9.
29. Gurbuz N, Kahraman N, Sonmez HE, Mokhlis HA, Kosar PA, Ozpolat B. MiRNA-193b-5p suppresses pancreatic cancer cell proliferation, invasion, epithelial mesenchymal transition, and tumor growth by inhibiting eEF2K. Anticancer Agents Med Chem. 2022. https://doi.org/10.2174/1871520622666220117123213.
30. Hamurcu Z, Sener EF, Taheri S, Nalbantoglu U, Kokcu ND, Tahtasakal R, et al. MicroRNA profiling identifies Forkhead box transcription factor M1 (FOXM1) regulated miR-186 and miR-200b alterations in triple negative breast cancer. Cell Signal. 2021. https://doi.org/10.1016/j.cellsig.2021.109979.
31. Hamurcu Z, Delibaşı N, Geçene S, Şener EF, Dönmez-Altuntaş H, Özkul Y, et al. Targeting LC3 and Beclin-1 autophagy genes suppresses proliferation, survival, migration and invasion by inhibition of Cyclin-D1 and uPAR/Integrin β1/Src signaling in triple negative breast cancer cells. J Cancer Res Clin Oncol. 2018. https://doi.org/10.1007/s00432-017-2557-5.
32. Ünlü Endirlik B, Bakır E, Ökçesiz A, Güler A, Hamurcu Z, Eken A, et al. Investigation of the toxicity of a glyphosate-based herbicide in a human liver cell line: Assessing the involvement of Nrf2 pathway and protective effects of vitamin E and α-lipoic acid. Environ Toxicol Pharmacol. 2022. https://doi.org/10.1016/j.etap.2022.103999.
33. Tunc CU, Kursunluoglu G, Akdeniz M, Kutlu AU, Han MI, Yerer MB, et al. Investigation of gold nanoparticle naproxen-derived conjugations in ovarian cancer. ACS Mater Au. 2023. https://doi.org/10.1021/acsmaterialsau.3c00033.
34. Wu P, Heins ZJ, Muller JT, Katsnelson L, de Bruijn I, Abeshouse AA, et al. Integration and analysis of CPTAC proteomics data in the context of cancer genomics in the cBioPortal. Mol Cell Proteomics. 2019. https://doi.org/10.1074/mcp.TIR119.001673.
35. Hamurcu Z, Kahraman N, Ashour A, Ozpolat B. FOXM1 transcriptionally regulates expression of integrin β1 in triple-negative breast cancer. Breast Cancer Res Treat. 2017;163:485–93. https://doi.org/10.1007/s10549-017-4207-7.
36. Yao S, Fan LY, Lam EW. The FOXO3-FOXM1 axis: A key cancer drug target and a modulator of cancer drug resistance. Semin Cancer Biol. 2018. https://doi.org/10.1016/j.semcancer.2017.11.018.
37. Vlachos IS, Zagganas K, Paraskevopoulou MD, Georgakilas G, Karagkouni D, Vergoulis T, et al. DIANA-miRPath v3.0: deciphering microRNA function with experimental support. Nucleic Acids Res. 2015. https://doi.org/10.1093/nar/gkv403.
38. Tong Z, Cui Q, Wang J, Zhou Y. TransmiR v2.0: an updated transcription factor-microRNA regulation database. Nucleic Acids Res. 2019. https://doi.org/10.1093/nar/gky1023.
39. Sadeghipour N, Kumar SU, Massoud TF, Paulmurugan R. A rationally identified panel of micrornas targets multiple oncogenic pathways to enhance chemotherapeutic effects in glioblastoma models. Sci Rep. 2022. https://doi.org/10.1038/s41598-022-16219-x.
40. levance of circulating MiRNA-21 and MiRNA-181 in prediction of glioblastoma multiforme prognosis. Arch Physiol Biochem. (2022). https://doi.org/10.1080/13813455.2020.1739716.
41. Sippl C, Teping F, Ketter R, Braun L, Tremmel L, Schulz-Schaeffer W, et al. The influence of distinct regulatory miRNAs of the p15/p16/RB1/E2F pathway on the clinical progression of glioblastoma multiforme. World Neurosurg. 2019. https://doi.org/10.1016/j.wneu.2019.07.134.
42. Gheidari F, Arefian E, Saadatpour F, Kabiri M, Seyedjafari E, Teimoori-Toolabi L, et al. The miR-429 suppresses proliferation and migration in glioblastoma cells and induces cell-cycle arrest and apoptosis via modulating several target genes of ERBB signaling pathway. Mol Biol Rep. 2022. https://doi.org/10.1007/s11033-022-07903-2.
43. Wang S, Wang W, Han X, Wang Y, Ge Y, Tan Z. Dysregulation of miR484-TUSC5 axis takes part in the progression of hepatocellular carcinoma. J Biochem. 2019. https://doi.org/10.1093/jb/mvz034.
44. Zhuang Z, Sun C, Gong H, High serum miR-484 expression is associated with the diagnosis and prognosis of patients with non-small cell lung cancer.Exp Ther Med. (2019). https://doi.org/10.3892/etm.2019.8010.
45. Shi W, Dong F, Jiang Y, Lu L, Wang C, Tan J, et al. Construction of prognostic microRNA signature for human invasive breast cancer by integrated analysis. Onco Targets Ther. 2019. https://doi.org/10.2147/OTT.S189265.
46. Zearo S, Kim E, Zhu Y, Zhao JT, Sidhu SB, Robinson BG, et al. MicroRNA-484 is more highly expressed in serum of early breast cancer patients compared to healthy volunteers. BMC Cancer. 2014. https://doi.org/10.1186/1471-2407-14-200.
47. Tahtasakal R, Hamurcu Z, Oz AB, Balli M, Dana H, Gok M, et al. miR-484 as an "OncomiR" in breast cancer promotes tumorigenesis by suppressing apoptosis genes. Ann Surg Oncol. 2025. https://doi.org/10.1245/s10434-024-16656-0.
48. Volinia S, Croce CM. Prognostic microRNA/mRNA signature from the integrated analysis of patients with invasive breast cancer. Proc Natl Acad Sci U S A. 2013. https://doi.org/10.1073/pnas.1304977110.
49. Mei Q, Xue G, Li X, Wu Z, Li X, Yan H, et al. Methylation-induced loss of miR-484 in microsatellite-unstable colorectal cancer promotes both viability and IL-8 production via CD137L. J Pathol. 2015. https://doi.org/10.1002/path.4525.
50. Shen Y, Qi L, Li Y, Zhang Y, Gao X, Zhu Y, et al. The downregulation of lncRNA pgm5-as1 inhibits the proliferation and metastasis via increasing miR-484 expression in colorectal cancer. Cancer Biother Radiopharm. 2021. https://doi.org/10.1089/cbr.2019.3059.
51. Qin J, Zhu T, Wu W, Chen H, He Y. Long non-coding RNA PCED1B-AS1 promotes the progression of clear cell renal cell carcinoma through miR-484/ZEB1 axis. Onco Targets Ther. 2021. https://doi.org/10.2147/OTT.S270149.
52. Paulus W, Baur I, Beutler AS, Reeves SA. Diffuse brain invasion of glioma cells requires beta 1 integrins. Lab Invest. 1996;75:819–26.
53. Virga J, Bognár L, Hortobágyi T, Zahuczky G, Csősz É, Kalló G, et al. Prognostic role of the expression of invasion-related molecules in glioblastoma. J Neurol Surg A Cent Eur Neurosurg. 2017. https://doi.org/10.1055/s-0036-1584920.
54. Namba N, Chonan Y, Nunokawa T, Sampetrean O, Saya H, Sudo R. Heterogeneous glioma cell invasion under interstitial flow depending on their differentiation status. Tissue Eng Part A. 2021. https://doi.org/10.1089/ten.TEA.2020.0280.
55. Munoz JL, Walker ND, Mareedu S, Pamarthi SH, Sinha G, Greco SJ, et al. Cycling quiescence in temozolomide resistant glioblastoma cells is partly

explained by microRNA-93 and -193-mediated decrease of Cyclin D. Front Pharmacol. 2019. https://doi.org/10.3389/fphar.2019.00134.
56. Xavier MA, Rezende F, Titze-de-Almeida R, Cornelissen B. BRCAness as a biomarker of susceptibility to PARP inhibitors in glioblastoma multiforme. Biomolecules. 2021. https://doi.org/10.3390/biom11081188.
57. Cruz Da Silva E, Mercier MC, Etienne-Selloum N, Dontenwill M, Choulier L. A systematic review of Glioblastoma-targeted therapies in phases II, III, IV clinical trials. Cancers (Basel). 2021. https://doi.org/10.3390/cancers13081795.
58. Ye L, Gu L, Wang Y, Xing H, Li P, Guo X, et al. Identification of TMZ resistance-associated histone post-translational modifications in glioblastoma using multi-omics data. CNS Neurosci Ther. 2024. https://doi.org/10.1111/cns.14649.
59. Prior C, Perez-Gracia JL, Garcia-Donas J, Rodriguez-Antona C, Guruceaga E, Esteban E, et al. Identification of tissue microRNAs predictive of Sunitinib activity in patients with metastatic renal cell carcinoma. PLoS ONE. 2014. https://doi.org/10.1371/journal.pone.0086263.
60. Annovazzi L, Caldera V, Mellai M, Riganti C, Battaglia L, Chirio D, et al. The DNA damage/repair cascade in glioblastoma cell lines after chemotherapeutic agent treatment. Int J Oncol. 2015. https://doi.org/10.3892/ijo.2015.2963.
61. Tang JH, Yang L, Chen JX, Li QR, Zhu LR, Xu QF, et al. Bortezomib inhibits growth and sensitizes glioma to temozolomide (TMZ) via down-regulating the FOXM1-Survivin axis. Cancer Commun. 2019. https://doi.org/10.1186/s40880-019-0424-2.
62. Garrett M, Fujii Y, Osaka N, Ito D, Hirota Yo, Sasaki Atsuo T, Emerging Roles of Wild-type and Mutant IDH1 in Growth, Metabolism and Therapeutics of Glioma. (In: Debinski W, editor. Gliomas [Internet]. Brisbane (AU): Exon Publications, 2021) . Chapter 4.
63. Maus A, Peters GJ. Glutamate and α-ketoglutarate: key players in glioma metabolism. Amino Acids. 2017. https://doi.org/10.1007/s00726-016-2342-9.
64. Kayabolen A, Yilmaz E, Bagci-Onder T. IDH mutations in glioma: double-edged sword in clinical applications ? Biomedicines. 2021. https://doi.org/10.3390/biomedicines9070799.

Publisher's Note